HEART RATE VARIABILITY ANALYSIS FROM PHOTOPLETHYSMOGRAPHY DURING RESTING AND EXERCISE

TICK SENGTHIPPHANY

A THESIS SUBMITTED IN PARTIAL FULFILLMENT

OF THE REQUIREMENTS FOR THE DEGREE OF

MASTER OF ENGINEERING IN COMPUTING IN ENGINEERING SYSTEMS

INTERNATIONAL COLLEGE

KING MONGKUT'S INSTITUTE OF TECHNOLOGY LADKRABANG

2015

KMITL-2014-IC-M-011-005

HEART RATE VARIABILITY ANALYSIS FROM PHOTOPLETHYSMOGRAPHY DURING RESTING AND EXERCISE

TICK SENGTHIPPHANY

THESIS SUBMITTED IN PARTIAL FULFILLMENT
OF THE REQUIREMENT FOR THE DEGREE OF
MASTER OF ENGINEERING IN COMPUTING IN ENGINEERING SYSTEM
INTERNATIONAL COLLEGE
KING MONGKUT'S INSTITUTE OF TECHNOLOGY LADKRABANG
2015

KMITL-2014-IC-M-011-005

THESIS TITLE	HEART RATE VARIABILITY ANALYSIS FROM PHOTOPLETHYSMOGRAPHY DURING RESTING AND EXERCISE
STUDENT NAME	MISS TICK SENGTHIPPHANY
STUDENT ID	56610018
DEGREE	MASTER OF ENGINEERING
PROGRAM	COMPUTING IN ENGINEERING SYSTEM
ADVISOR	DR. SURADEJ TRETRILUXANA

ABSTRACT

Heart Rate Variability (HRV) is well known to be the measure of cardiac autonomic function. The two branches of systemic control, sympathetic and parasympathetic (vagal) modulations, are reflected in the variation of heart beat interval in Electrocardiogram (ECG). And it could be used as a noninvasive marker in monitoring the physiological state of an individual. The aim of this thesis is to investigate the possibility of computing Heart Rate Variability indices from the finger Photople-thysmogram (PPG). To indicate that whether Pulse Rate Variability from PPG signal can be used as an alternative to Heart Rate Variability from the ECG signal in both resting and exercise conditions. The PPG and ECG signals from 33 participants were recorded simultaneous-sly during resting and exercise conditions. The peaks of PPG and R-waves of ECG were detected and reconstructed to the Peak-to-Peak interval (PPI) and R-to-R interval (RRI) waveforms respectively. In both conditions, the mean and standard deviation (SDNN) of the intervals over 5 minutes were computed from the two waveforms. Results from cross correlation between PPI and RRI show that the average correlation coefficients (r) are higher in resting than exercise. In regression analysis of the statistical parameters between RRI and PPI, the determination coefficients (R^2) of the means are close to one in both conditions, whereas the R^2 of SDNN in exercise is lower than the one in resting. The inconsistent value, R^2 of mean and SDNN, during exercise is the consequence of poor PPG and ECG signal quality causing the lower value of R^2. However, it can be significant because the value of R^2 is the closest to the line of best fit. This finding suggests that the HRV indices can be evaluated from PPG with reliability during resting and exercise.

ACKNOWLEDGEMENTS

First of all, I would like to sincerely thank my advisor Dr. Suradej Tretriluxana who gave me guidance and direction that was needed to complete this thesis. Without his generous help, this thesis would not have been possible.

I would like to acknowledgement ASEAN University Network/Southeast Asia Engineering Education Development Network (AUN/SEED-Net) and King Mongkut's Institute of Technology Ladkrabang Research Fund for awarding me the scholarship with the financial support for master degree for two years. Furthermore, I extend my sincere appreciation to King Mongkut's Institute of Technology Ladkrabang for giving me the great opportunity to do research in a warm and friendly environment.

I gratefully acknowledge goes also to all professors, lecturers and supporting staffs in King Mongkut's Institute of Technology Ladkrabang, especially International College (IC), who always help and give me guidelines and convenience during the whole period of my master studies.

Thank you to Asst. Dr. Kitiphol Chitsakul and the Biomedical Measurement and Computation Laboratory's (BMCL) member in Electronics Department, King MongKut's Institute of Technology Ladkrabang and volunteers for supporting the Biopac Measurement System and time to measure the Electrocardiogram (ECG) Photoplethy-smogram (PPG) and Respiration signals.

Finally, I would like to thank to my family and friends for their constant encouragement during my studies.

Tick Sengthipphany

TABLE OF CONTENTS

TABLE OF CONTENTS (CONTINUE)

LIST OF TABLES

LIST OF FIGURES

LIST OF FIGURES (CONTINUE)

CHAPTER 1
INTRODUCTION

1.1 Introduction

The Heart Rate Variability (HRV) plays a critical role in neurophysiology, especially when analyzing data from the Electrocardiogram (ECG). Many people have expressed interest in studying HRV signals. Our "Biomedical Measurement and Computation Laboratory (BMCL)" has a long history of studying HRV analyzes [1-2], for example the study of HRV in the stress of an animal. The study shows some significant from the analyzed signals. Thus, we propose to apply the HRV analyses to study the stress of human. An improved HRV methodology for analyzing the ECG was developed to compute the average of R-to-R Interval (RRI) by analyzing both Time and Frequency Domains [3]. The main focus of the study is to understand the HRV in human stress and subsequently learn how to manage the stress [4].

Stress is a condition that the human body and mind activates to respond to pressure and threat. Stress may also produce when compelling the human body and mind in response to events. Stress can induce headaches, migraines and eyestrain [5]. HVR may reflect changes in body stress [6]. Therefore, HVR analysis is commonly used as a quantitative analysis to depict the activity of autonomic nervous system (ANS), through calculating and estimating noninvasive biochemical and medical. Many researchers have succeeded and recognized in the studies of ECG of human. In this study, ectopic events [7] and death in heart or diabetic neuropathy patients are forecasted [8].

In this study, first, the HRV analysis in human stress was conducted using ECG signal and saliva. The preliminary analysis produced negative results (not support the hypothesis). This is due to the fact that subject stress analysis cannot be experimented.

Due to the aforementioned results, it is recognized that the study should focus on correlation of HRV from Photoplethysmogram (PPG) with ECG at rest and exercise conditions. For heart rate, PPG acts as a surrogate of ECG. Because it is more convenient to measure PPG than an ECG, the study focuses on measuring PPG. In this study, we measured the time domain and frequency domain of peak to peak interval of PPG and its square coherence to the time domain and frequency domain with HRV from ECG in resting and exercise. The results showed that the time domain and frequency domain of

PPG correspond almost well with HRV, especially in the healthy subjects at rest. However, the correlation is decreased in stimulus conditions such as exercise.

1.2 Background and Problem Statement

Noninvasive biomedical monitoring and noninvasive medical diagnosis are preferred, whenever possible, to avoid the risks and expenses associated with surgical opening of the body surface, e.g., infection, adverse systemic reactions to anesthesia, dye injections, antibiotics and other medications, and surgical errors. Visual assessments of physiological parameters are very attractive since they often provide simple, noninvasive, and continuous physiological monitoring conditions. Nowadays, physiological signals can be accurately obtained and recorded by means of optical instruments, which supply researchers and doctors with important information as a basis for diagnosis and treatment. PPG is such a simple and low-cost optical technique that allows noninvasively detecting blood volume changes in the microvascular bed of tissue. The most recognized waveform features are the peripheral pulse, and it is synchronized to each heartbeat. It is generally accepted that the PPG signal can provide valuable information about the cardiovascular system [9].

Heart rate variability has been extensively studied in the electrocardiogram (ECG) signals. HRV has become the conventionally accepted term to describe variations of both instantaneous heart rate and RR intervals in the electrocardiogram signals. Therefore, a number of terms have been used in the literature to describe HRV, for example, cycle length variability, heart period variability, and RR variability.

The single largest cause of premature death in the developed world today is heart and circulatory disease. Unfortunately, conditions associated with heart and circulatory disease can go unnoticed for a long time before they suddenly manifest themselves, with potentially lethal results. If these conditions had been detected earlier, lives would be saved and many tragedies could have been avoided. Unfortunately, today, detecting the early signs of heart diseases requires invasive and expensive observation performed over a long period of time, usually by a medical professional. Even then, due to the conditional nature of such a disease, and the erratic nature of the symptoms, there is no guarantee of detection.

Evaluation of visual of physiological parameters is very attractive because they often provide simple, non-invasive, and continuous physiological monitoring conditions.

Photoplethysmography is such a convenient optical technique and can continuously record the light intensity scattered from a given source by the tissue and collected by a suitable photodetector. The arterial pulse waveform carries physiological information about the mechanical properties of the peripheral arteries, and thus the PPG pulse wave could be used to noninvasively assess artery stiffness. A pulsatile PPG signal reveals the heart rate (HR) and could be used to study heart rate variability.

1.3 Objective of the Study

The specific aims of this thesis are:

- To analysis heart rate variability from photoplethysmography during resting and exercise.
- To evaluate the cross correlation between two waveforms during resting and exercise conditions.

1.4 Methodology

1. The beat-to-beat interval waveforms extracted from ECG peak-to-peak interval waveforms extracted from PPG were generated.
2. Analysis heart rate variability from ECG and PPG signals.
3. The cross correlation between two waveforms were evaluated during resting and exercise conditions.
4. Computed time domain and frequency domain statistical parameters of HRV from PPG and ECG signals. Finally, all parameters were compared through the use of regressing analysis.

1.5 Scope of the Study

This research focuses on Heart Rate Variability Analysis by using time domain and frequency domain analysis. The ECG and the PPG signals are extracted from the experiment. The data are collected in the computer database during the 10 minutes of resting and 15 of exercise.

For each trial, the two 5-minute portion of PPG and ECG were selected from resting and exercise conditions for analysis. Due to the poor signal quality, four subject's data were removed from the analysis in exercise conditions. All peaks of PPG and R-waves of ECG were detected and reconstructed to Peak-to-Peak and R-to-R interval time

series respectively. The cross correlations between these two time series were performed and two average correlation coefficients (r) and determination coefficients (R^2) were computed across subjects in resting (n=33) and exercise (n=29) conditions. For the process and methodology of analyzing heart rate variability, Labview program is used for this research.

1.6 Organization of the thesis

This thesis is organized as follows:

Chapter 1 begins by introducing research background, including a research problem statement, research objectives, methodology, and the scope of the research. Chapter 2 introduces ECG signals and several techniques used in HRV analysis. Chapter 3 presents the basic aspects of the PPG technique, the basis for understanding the principle of PPG. A brief review of the early and recent history of PPG is included. Next, the PPG measurement system is described. Finally, Photoplethysmographic applications in clinical physiological measurements are presented. Chapter 4 states the experimental system, such as the experimental setup and protocol. Chapter 5 presents the results of the experiment. Chapter 6 concludes and discusses the work carried out

CHAPTER 2
ELECTROCARDIOGRAM SIGNAL

This chapter introduces the electrocardiogram signal and other several techniques used in HRV analysis.

2.1 Physiology of the Heart in Human

The heart is one of the most critical organs in the human body, thus the development of methods for monitoring its functionality is crucial. Electrocardiography is considered to be one of the most powerful diagnostic tools in medicine that is routinely used for the assessment of the functioning of the heart.

The human heart is controlled by a series of electrical discharges from specific localized nodes within the myocardium (cardiac muscle). These discharges propagate through the cardiac muscle and stimulate contractions in a coordinated manner in order to pump deoxygenated blood via the lungs (for oxygenation) and back into the vascular system. The physical action of the heart is therefore induced by a local periodic electrical stimulation. As a result of the latter, a change in the potential of the order of 1mV can be measured during the cardiac cycle between two surface electrodes attached to the patient's upper torso (usually either side of the heart). This signal is known as the electrocardiogram (ECG).

In a normal heart, each beat begins with the stimulation of the sinoatrial (SA) node, high up in the right atrium which causes depolarization of the cardiac muscle in this locality. This stimulation is both regular and spontaneous and is the source of the primary pacemaker within the heart with an intrinsic frequency of 70 to 120 beats per minute (BPM). The impulse spreads from the SA node to depolarize the atria (the upper two cavities). The electrical signal, then reaches the atrioventricular (AV) node, located in the right atrium. Normally, an impulse can only reach the ventricles via the AV node since the rest of the myocardium is separated from the ventricles by a non-conducting fibrous ring. As the AV node is activated, it momentarily delays conduction to the rest of the heart and so acts as a safety mechanism by preventing rapid atrial impulses from spreading to the ventricles at the same rate. If the AV node fails to receive impulses it will take over as the cardiac pacemaker (at a much lower frequency of 40 to 60 BPM). The SA node will inhibit the pacemaker whenever its impulses reach the AV node.

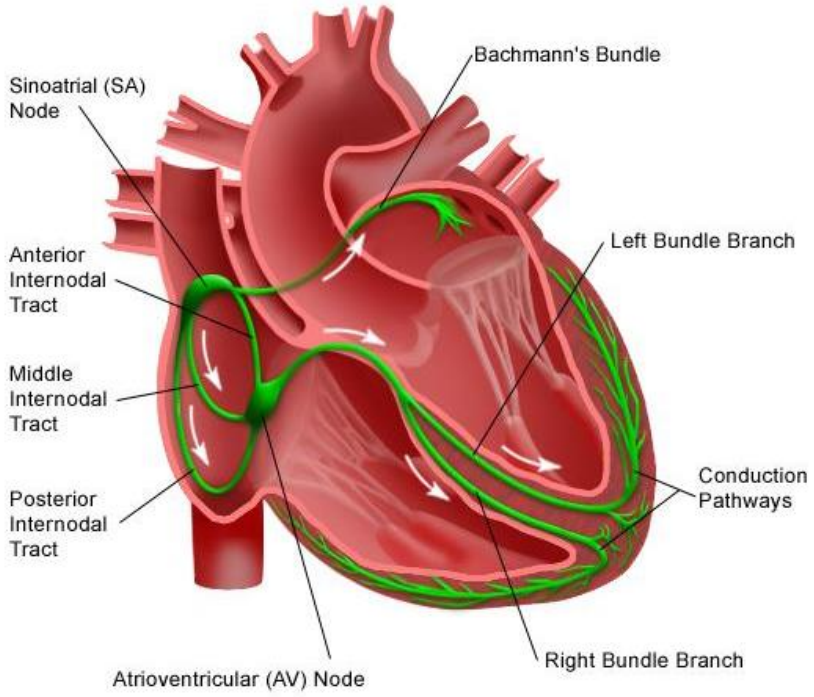

Figure 2.1 Source nodes of electrical stimulation within the heart [10].

Once the impulse has passed the AV node, it enters the bundle of his. This conducting network spread out into the inter-ventricular septum and divides into left and right bundle branches. As the impulse moves through this region and into the posterior and anterior fascicles, it stimulates depolarization of the ventricles. There is a ventricular pacemaker (with a beat frequency of 15 to 40 BPM), which takes over as the main pacemaker if the AV node fails. After the depolarization of the ventricles, a transient period follows, where no further ionic current can be flown through the myocardium. This is known as the refractory period and lasts at least 200 ms. There is then a recharging (repolarization) of the ventricular myocardium to its resting electrical potential and the heart is then ready to repeat the cycle as show in Figure 2.1

The electrocardiogram is the conventional method for noninvasive interpretation of the electrical activity of the heart in real-time. The electrical cardiac signals are recorded by an external device, by attaching electrodes to the outer surface of the skin of the patient's thorax. These currents stimulate the cardiac muscle and cause the contractions and relaxations of the heart [5]. The electrical signals travel through the electrodes to the ECG device, which records them as characteristic waves. Different waves reflect the activity of different areas of the heart, which generate the respective

flowing electrical currents. Figure 2.2 shows a schematic representation of a normal ECG and its various waves.

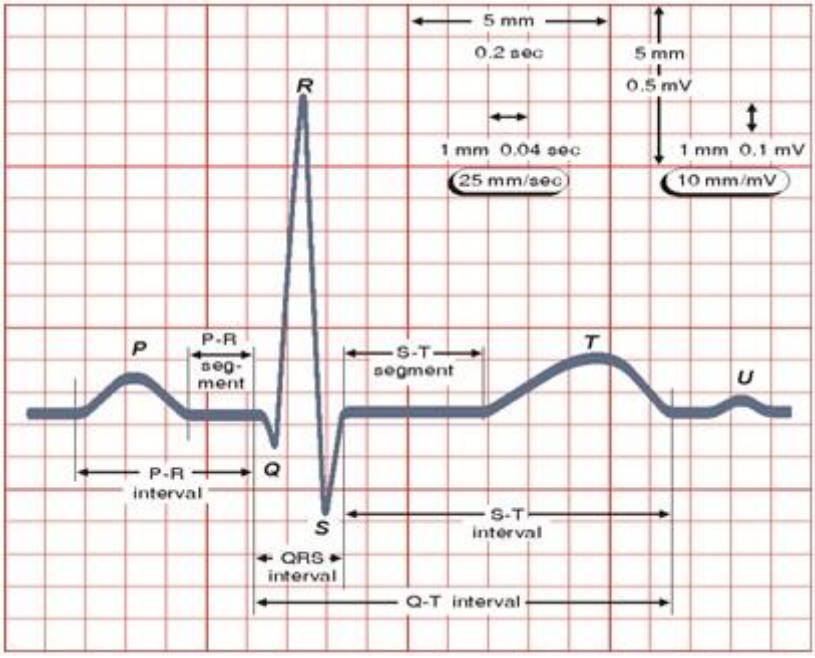

Figure 2.2 The normal electrocardiogram [10].

The electrocardiogram is composed of waves and complexes; in the normal sinus rhythm are comprised of the P wave, PR Interval, PR Segment, QRS Complex, ST Segment, QT Interval and T wave.

P wave

P waves are caused by atrial depolarization. In normal sinus rhythm, the SA node acts as the pacemaker. The electrical impulse from the SA node spreads over the right and left atrial depolarization. The P wave contour is usually smooth, entirely positive and uniform size. The P wave duration is normally less than 0.12 second and the amplitude is normally less o. 25 mV. A negative P-wave can indicate depolarization arising from the AV node.

The PR Segment

PR segment is the portion of the ECG wave from the end of the P wave to the beginning of the QRS complex, lasting about 0.1 second. The PR segment corresponds to

the time between the ends of atrial depreciation to the onset of ventricular depolarization. The PR segment is an isoelectric segment, that is, no wave or deflection is recorded. During the PR segment, the impulse travels from the AV node through the conducting tissue (bundle branches, and Purkinje fibers) towards the ventricles. (Note a wave will be recorded only after the impulses exit the conducting systems and activates the ventricular muscle to give the QRS complex). Most of the delay in the PR segment occurs in the AV node.

The QRS Complex

In normal sinus rhythm, each P wave is followed by a QRS complex. The QRS complex represents the time it takes for depolarization of the ventricles. Activation of the anteriosetal region of the ventricular myocardium corresponds to the negative Q wave. The Q wave is not always present. Activation of the rest of ventricular muscle of the endocardial surface corresponds to the rest of the QRS wave. The R wave is the point when half of the ventricular myocardium has been depolarized. Activation of the posteriobasal portion of the ventricles gives the RS line. The normal QRS duration range is from 0.04 second to 0.12 second measured from the initial deflection of the QRS from the isoelectric line to the end of the QRS complex.

The ST Segment

The ST segment represents the period from the end of ventricular depolarization to the beginning of ventricular depolarization. The ST segment lies between the end of the QRS complex and the initial deflection of the T-wave and is normally isoelectric. It is clinically important if elevated or depressed as it can be a sign of ischemia and hyperkalemia.

The QT Interval

The QT interval begins at the onset of the QRS complex and with the end of the T wave. It represents the time between the start of ventricular depolarization and the end of ventricular depolarization. It is useful as a measure of the duration of repolarization. The QT interval will vary depending on the heart rate, age and gender. It increases with bradycardia and decreases with tachycardia. Men have shorter QT intervals (0.39 second) than women (0.41 second). The QT interval is influenced by electrolyte balance, drugs, and ischemia.

The T wave

The T wave corresponds to the rapid ventricular depolarization. The T wave is normally rounded and positive. The T wave can become inverted, peaked or flattened due to electrolyte imbalance, hyperventilation, ischemia or myocardial infarction.

2.2 ECG Recording

ECG is the recording from the body surface of the electrical activity generated by the heart. ECG has provided an important noninvasive means of recording and detecting each cardiac cycle. The electrical signals within the heart are of relatively small amplitude, in the range of 100 mV. Since the inside of the human body consists of electrically conductive tissues, a part of the cardiac contraction signal is carried to the skin, where it can be detected by an ECG. On the skin, the signals are much lower in amplitude than at the heart, approximately 1 mV. However, these signals at the skin surface can be amplified and filtered sufficient to provide a clear representation of original signals from the heart.

In order to record an ECG waveform, a different recording between two points on the body is made. Traditionally, each differential recording is referred to as a lead. The original Lead I, II and III ECG electrode placements were defined by Garcia in 2001 [11]. The electrode placement, called Einthoven's triangle, is still used today for routine ECG measurement. Electrodes are placed on the left leg (on the sign above the foot), on the right arm (about one quarter of the way from the wrist on the medial surface) and on the left arm in the same location. The potentials at these body locations is denoted: V_{LL}, V_{RA} and V_{LA}, respectively. ECG lead I is the potential between the left arm (+) and the right arm (-), i.e. $V_I = V_{LA} - V_{RA}$. Lead II is taken between the left leg (+) and the right arm (-), i.e. $V_{II} = V_{LL} - V_{RA}$, and Lead III is between the left leg (+) and the left arm (-), i.e. $V_{III} = V_{LL} - V_{LA}$. Because the body is assumed to be purely resistive at ECG frequencies, the four limbs can be thought of as wires attached to the torso. Hence, lead I could be recorded from the respective shoulders without a loss of cardiac information. Today, 12-lead ECG (using 10 electrodes) consist of six limb leads and six chest leads, provides discriminatory information for diagnosing abnormalities in the pacing and the conduction system of the heart. Figure 2.3 Illustrates the 12-lead set.

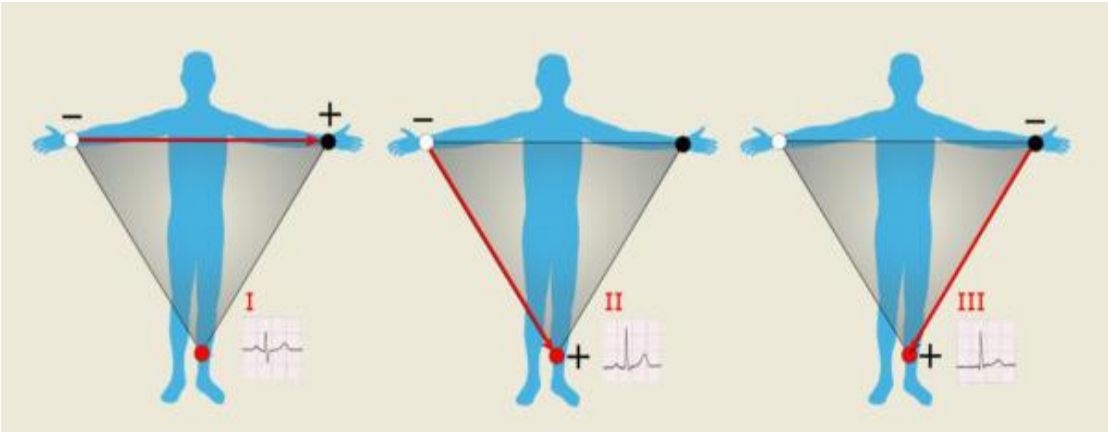

$$I = V_{LA} - V_{RA} \qquad II = V_{LL} - V_{RA} \qquad III = V_{LL} - V_{LA}$$

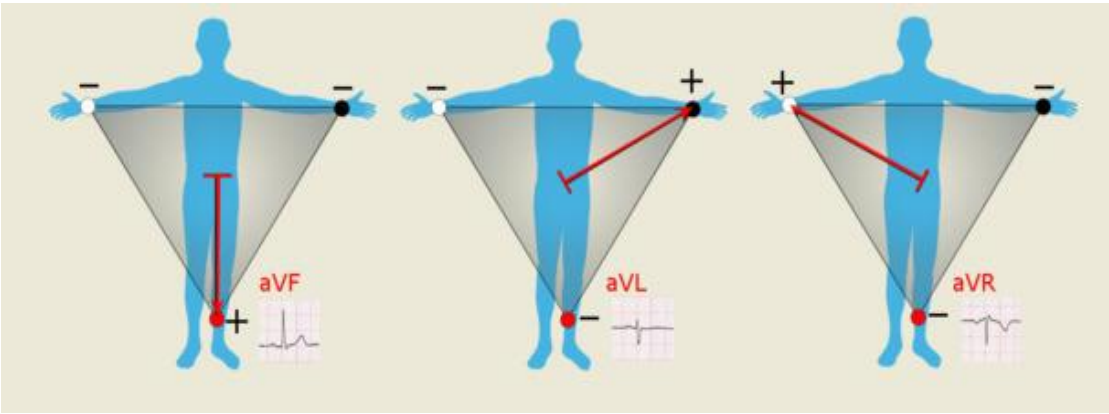

$$aVF = \frac{2V_{LL} - V_{LA} - V_{RA}}{2} \qquad aVL = \frac{2V_{LA} - V_{RA} - V_{LL}}{2} \qquad aVF = \frac{2V_{RA} - V_{LA} - V_{LL}}{2}$$

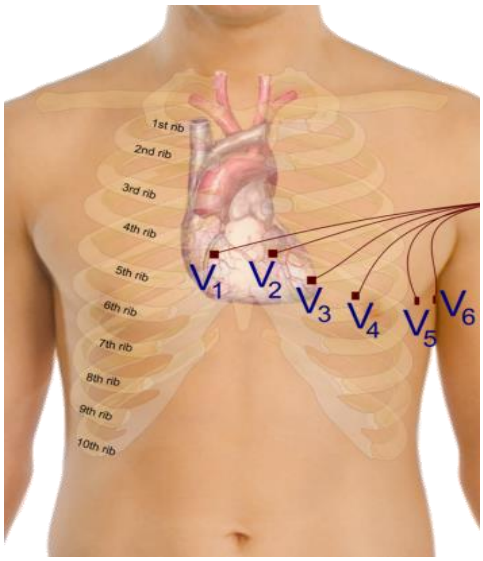

$$V_t = u_i - V_w \quad / \quad i = 1 \text{ to } 6$$

Figure 2.3 The 12-lead ECG is formed by the 3 bipolar surface leads: I, II, and III the augmented Wilson terminal referenced limb leads: aVR, aVL, and aVF the Wilson terminal referenced chest leads: V1, V2, V3, V4, V5 and V6 [11].

2.3 Heart Rate Variability

It is generally known that the change in autonomic nervous system is related to physiological situations as well as various pathological conditions. ANS assessments have been presented, for instance, cardiovascular reflex test [12], biochemical [13] and scintigraphic tests [14]. Direct measures or invasive assessments are not routinely used. Several noninvasive markers such as HRV [15], baroreflex sensitivity (BRS) [16], QT interval (Schwartz and Wolf 1978) [17] and heart rate turbulence (HRT) in 1999 [18] have been suggested. Based on simplicity and variety of calculations, HRV is the most accepted evaluations of sympathovagal regulation in ANS. HRV is defined as a noninvasive electrocardiographies marker reflecting ANS activity in two branches; sympathetic and parasympathetic [19]. The development of HRV can be traced back to 1965 in the note of Hon and Lee [7] on the fetal heart rate patterns. The application of HRV as the risk indicator is first published in 1978 by Wolf et al [8].

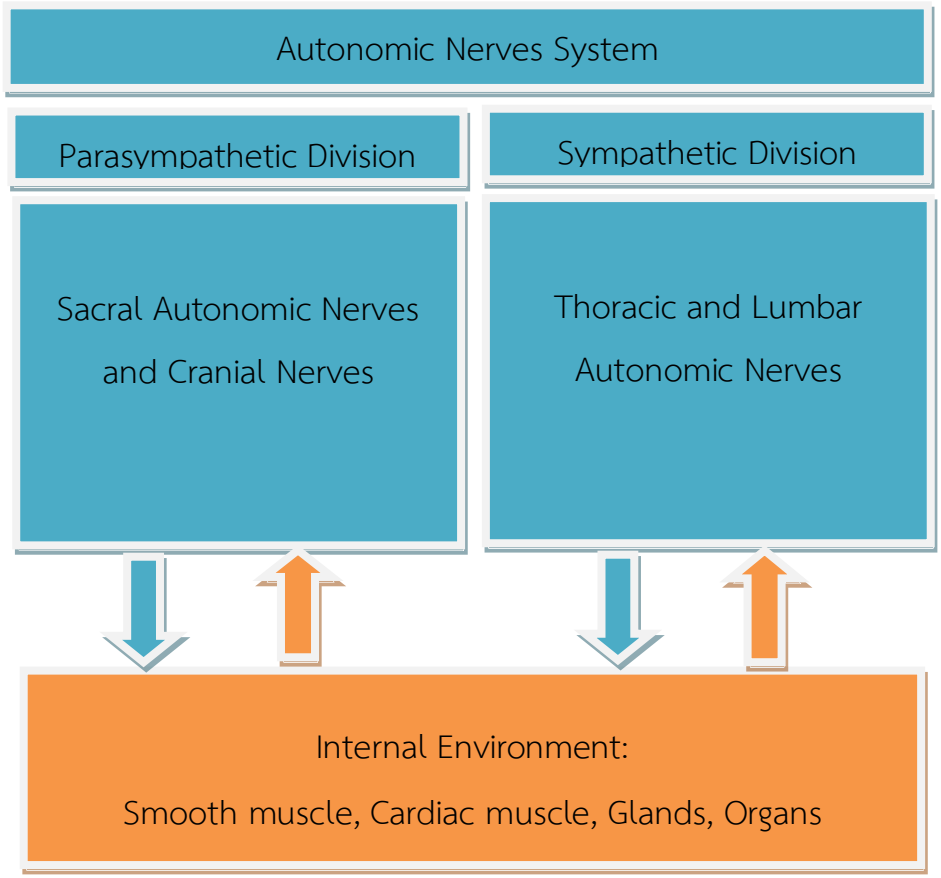

Figure 2.4 Influences of Sympathetic and Parasympathetic activities in the autonomic nervous system.

The autonomic nervous system, or ANS, is the portion of the nervous system that regulates involuntary processes. In other words, these are processes that are not under conscious control. The ANS is divided into two divisions: the parasympathetic and the sympathetic nervous systems in Figure 2.4

Because of the popularity of the HRV analysis, the European Society of Cardiology (ESC) and the North American Society of Pacing and Electrophysiology (NASPE) established the standards of measurements and physiological interpretation of HRV in 1996 (Task Force of the European Society of Cardiology and the North American Society of Pacing and Electrophysiology 1996) [3]. They classified the measurement of HRV into three domains and our research use two methods for analysis such as: Time domain methods, Frequency domain methods.

In addition HRV analysis from ECG, The PPG has been considered as a promising surrogate for ECG in measuring heart rate variability. However, there is a dispute on validity of HRV information provided by PPG pulse intervals. On one hand, high correlation between pulse intervals and RR intervals (RRI) were obtained in some studies and it was concluded that pulse variability can serve as an alternative approach to obtain HRV information [20-21].

2.3.1 Time Domain Methods

Variations in heart rate may be evaluated by a number of methods. Perhaps the simplest to perform are the time domain measures. With these methods either the heart rate at any point in time or the intervals between successive normal complexes are determined. In a continuous electrocardiographic record, each QRS complex is detected, and the so-called normal-to-normal (NN) intervals (that is all intervals between adjacent QRS complexes resulting from sinus node depolarization, or the instantaneous heart rate is determined. Simple time domain variables that can be calculated include the mean NN interval, the mean heart rate, the difference between the longest and shortest NN interval, the difference between night and day heart rate, etc. Other time domain measurements that can be used are variations in the instantaneous heart rate secondary to respiration, tilt, Valsalva maneuver, or secondary to phenylephrine infusion. These differences can be described as either differences in heart rate or cycle length. Usually the RR interval in QRS complexes are detected the indices in this group are generated by performing simple mathematical or statistic calculation on those time series, such as the mean RR interval,

standard deviation of HRV. Examples of Time domain used indices are given in Table 2.1

Table 2.1 Example of some Time domain parameters

Parameter Name	Units	Description
MeanRR	ms	Mean of 5-minute RR interval
SDNN	ms	Standard deviation of all NN intervals
CC (r)		Correlation coefficient
DC (R^2)		Determination coefficient

RR Interval Calculation

Heart rate variability analysis in this thesis brings from the RR interval of ECG signals. For peak detector, is finding the location in time series $t_{(i)}$, and second derivative of peaks in the input signal. $(i = 1, 2, 3, ..., n)$, use the following equation:

$$RR_i = t_{(i)} - t_{(i-1)} \tag{2.1}$$

The time-domain methods are the simplest to perform since they are applied straight to the series of successive RR interval values. The most evident, such measure is the mean value of RR intervals or, correspondingly, the mean HR. In addition, several variables that measure the variability within the RR series exist. The standard deviation of RR intervals (SDNN) is defined as:

$$Mean = \frac{1}{N}\sum_{i=1}^{N} RR_i \tag{2.2}$$

$$SDNN = \sqrt{\frac{1}{N-1}\sum_{i=1}^{N}(RR_i - RR_{mean})^2} \tag{2.3}$$

Where RR_i denotes the value of i the RR interval and N is the total number of successive intervals.

Correlation coefficient (CC) r always is in the interval [–1, 1]. If correlation coefficient r is 1, x and y have a complete positive correlation. In other words, the data points from x and y lie on a perfectly straight, positively-sloped line. If correlation coefficient r is –1, x and y have a complete negative correlation. In other words, the data points from x and y lie on a perfectly straight, negatively-sloped line. If correlation coefficient r is 0, x and y have no correlation, n is sample size. The coefficient of determination (CD) is the ratio of the explained variation to the total variation. The coefficient of determination is such that $0 < R^2 < 1$, and show the strength of the linear association between x and y. The coefficient of determination represents the percent of the data that is the closest to the line of best fit. The linear correlation coefficient also is known as the Pearson's correlation. The following equation describes the linear correlation coefficient:

$$r = \frac{n(\sum xy) - (\sum x)(\sum y)}{\sqrt{[n(\sum x^2) - (\sum x^2)] \times [n(\sum y^2) - (\sum y^2)]}} \tag{2.4}$$

The coefficient of determination makes interpreting correlation coefficients easier. Notwithstanding its impressive name, calculating this coefficient is simple. The coefficient of determination is simply the squared value of the correlation coefficient.

2.3.2 Frequency Domain Methods

The time domain methods are computationally simple, but lack the ability to discriminate between sympathetic and parasympathetic contributions of HRV.

These studies of HRV employed a power spectral density (PSD) analysis providing the basic information of how power (i.e. variance) distributes as a function of frequency. The HR signal is decomposed into its frequency components and quantified in terms of their relative intensity (power). Methods for the calculation of PSD may be generally classified as non-parametric and parametric. In most instances, both methods provide comparable results. The advantages of the non-parametric methods are: (a) the simplicity of the algorithm employed (fast Fourier transform (FFT) in most of the cases) and (b) the high processing speed. But these methods, i.e. FFT, suffer from spectral leakage effects due to windowing. The spectral leakage leads to masking of weak signal that are present in the data. The parametric (model based) power spectrum estimation

methods avoid the problem of leakage and provide better frequency resolution than nonparametric or classical methods. The advantages of parametric methods are: (a) smoother spectral components which can be distinguished independently of preselected frequency bands, (b) easy post-processing of the spectrum with an automatic calculation of low and high frequency power components and easy identification of the central frequency of each component, and (c) an accurate estimation of PSD even on a small number of samples on which the signal is supposed to maintain stationary and we use Autoregressive (AR) method and Autoregressive Moving Average (ARMA) method for heart rate variability analysis. The basic disadvantage of parametric methods is the need to verify the suitability of the chosen model and its complexity (i.e. the order of the model).

The power spectrum of healthy subjects consists of four major frequency bands. They do not have fixed periods and the central frequencies may vary considerably. The limits for the spectral components usually used [22] are: high frequency (HF) component 0.15-0.4 Hz, low frequency (LF) component 0.04-0.15 Hz, very low frequency (VLF) component 0.003-0.04 Hz, and ultra-low frequency (ULF) component <0.003 Hz. The frequency domain measures of HRV are listed and described in Table 2.2

Table 2.2 Example of some frequency domain parameters

Variable	Units	Description	Frequency range
ULF	ms^2	Power in ultra-low frequency range	< 0.003 Hz
VLF	ms^2	Power in very low frequency range	0.003 - 0.04 Hz
LF	ms^2	Power in low frequency range	0.04 - 0.15 Hz
HF	ms^2	Power in high frequency range	0.15 - 0.4 Hz

1. Non-Parametric Method

The Fourier transform of data that needs to be derived from a simple of a random signal is bordered by the sampling rate.

$$f_s = \frac{sample}{\sec ond} = \frac{1}{T_s} \tag{2.5}$$

If the data $x_0, x_1, ..., x_{N-1}$ derived from random N data over time, as well as the conversion of data from the time domain to the frequency domain according to the equation.

$$X_n(f) = \Delta t \sum_{n=0}^{N-1} x_n e^{2\pi f n \Delta t} \tag{2.6}$$

Which $\Delta t = \frac{1}{f_s}$

f_s is sampling rate

X_n is the data of the time domain from sampling rate

n is the number of times the sampling (n= 0, 1, …)

$X_n(f)$ is a signal of the frequency domain

Which the frequency $f(Hz)$ of value in the range $-\frac{1}{2} \le f \le \frac{1}{2}$

Power spectral density function shows the strength of the variations (energy) as a function of frequency. In other words, it shows at which frequency variations are strong and at which frequency variations are weak. The unit of PSD is energy per frequency (width) and you can obtain energy within a specific frequency range by integrating PSD within that frequency range. Computation of PSD is done directly from the square of X_n, $|X_n|^2$ as this an equation.

$$S_n(f) = \sum_{n=0}^{N-1} |X_n|^2 \tag{2.7}$$

2. Parametric Method

The Parametric or model-based methods of spectral estimation assume that the signal satisfies a generating model with a known functional form, and then proceed by estimating the parameters in the assumed model. The signal's spectral characteristics of interest are then derived from the estimate model. In those cases where the assumed

model is a close approximation to the reality, it is no wonder that the pragmatic method provides more accurate spectral estimates the non-parametric techniques [23].

A rational PSD is a rational function of $e^{-j\omega}$

$$\phi(\omega) = \frac{\sum_{k=-m}^{m} \Upsilon k e^{-j\omega k}}{\sum_{k=-n}^{n} \rho k e^{-j\omega k}} \tag{2.8}$$

Where $\Upsilon - k = \Upsilon k*$ and $\rho - k = \rho k*$

The Weierstrass Theorem of calculus asserts that any continuous PSD can be approximated arbitrarily closely by rational PSD, provided the degrees m and n are chosen at large, that is the rational PSD from a dense set in the class of all continuous spectra, Since $\phi(\omega) \geq 0$, the rational spectral density can be factored as follows:

$$\phi(\omega) = \left| \frac{B(\omega)}{A(\omega)} \right|^2 \sigma^2 \tag{2.9}$$

Where σ^2 is a positive scalar, and $A(\omega)$, $B(\omega)$ are the polynomials

$$\begin{aligned} A(\omega) &= 1 + a_1 e^{-j\omega} + \ldots + a_n e^{-jn\omega} \\ B(\omega) &= 1 + b_1 e^{-j\omega} + \ldots + b_n e^{-jm\omega} \end{aligned} \tag{2.10}.$$

The result from equation (2.9) can similarly be expressed in the Z-domain. With the notation

$\phi(z) = \sum_{k=-m}^{m} \Upsilon k e^{-jzk} \; / \; \sum_{k=-n}^{n} \rho k e^{-jzk}$, The factor $\phi(z)$ as:

$$\phi(z) = \sigma^2 \frac{B(z)B*(\frac{1}{z^*})}{A(z)A*(\frac{1}{z^*})} \tag{2.11}$$

Where, for example $A(z)$ and $A*(\frac{1}{z^*})$ as:

$$A(z) = 1 + a_1 z^{-1} + ... + a_n z^{-n}$$
$$A*(\frac{1}{z}) = [A(\frac{1}{z^*})] = 1 + a_1 * z^{-1} + ... + a_n * z^{-n}$$

Use the substitution $z = e^{j\omega}$

The arbitrary rational PSD in equation (2.9) can be associated with a signal obtained filtering white noise of power σ^2 through the rational filter with transfer function

$$H(\omega) = \frac{B(\omega)}{A(\omega)} \tag{2.12}$$

Can be written in the time domain as

$$y(t) = \frac{B(z)}{A(z)} e(t) \tag{2.13}$$

Or, alternatively

$$A(z)y(t) = B(z)e(t) \tag{2.14}$$

Where $y(t)$ is the filter output, and z^{-1} is the unit delay operator $(z^{-k}y(t) = y(t-k))$.
$e(t)$ is white noise of variance equal to σ^2

Hence, by means of the spectral factorization theorem, the parameterized model of $\phi(\omega)$ turned into a model of the signal itself. The spectral estimation problem can then be reduced to a problem of signal modeling. In the following sections, present several methods for estimating the parameters in the signal model using the equation (2.14).

A signal $y(t)$ satisfying the equation (2.13) is called an autoregressive moving average (ARMA or ARMA (n, m)) signal. If m = 0, then $y(t)$ an autoregressive (AR or AR (n)) signal, and $y(t)$ is a moving average (MA or MA (m)) signal if n = 0. Which summarizes these naming conventions below:

$$ARMA: A(z)y(t) = B(z)e(t)$$
$$AR: A(z)y(t) = e(t)$$
$$MA: y(t) = B(z)e(t) \qquad (2.15)$$

Covariance Structure of ARMA Processes

Equation (2.14) can be written as

$$y(t) + \sum_{i=1}^{n} a_i r(k-i) = \sum_{j=0}^{m} b_j e(t-j) \quad / \ (b=0) \qquad (2.16)$$

Multiplying the equation (2.16) by $y^*(t-k)$ and taking expectation yields

$$r(k) + \sum_{i=1}^{n} a_i r(k-i) = \sum_{j=0}^{m} b_j E[e(t-j)y^*(t-k)] \qquad (2.17)$$

Since the filter $H(z) = \dfrac{B(z)}{A(z)}$ is asymptotically stable and causal, can write

$$H(z) = \frac{B(z)}{A(z)} = \sum_{k=0}^{\infty} h_k z^{-k} \quad (\mathrm{h}_0 = 1)$$

Which gives

$$y(t) = H(z)e(t) = \sum_{k=0}^{\infty} h_k e(t-k)$$

Then the term $E[e(t-j)y^*(t-k)]$ becomes

$$E[e(t-j)y^*(t-k)] = E[e(t-j)\sum_{s=0}^{\infty} h_s * e^*(t-k-s)]$$
$$= \sigma^2 \sum_{s=0}^{\infty} h_s * \delta_{j,k+s} = \sigma^2 h^*_{j-k}$$
$$h_k = 0, k < 0$$

Which use the convention that $h_k = 0, k < 0$. Thus, equation (2.17) becomes

$$r(k)+\sum_{i=1}^{n} a_i r(k-i)=\sigma^2\sum_{j=0}^{m} b_j h^*_{j-k} \tag{2.18}$$

In general, h_k is a nonlinear function of the $\{a_i\}$ and $\{b_i\}$ coefficient. However, since $h_s=0$ for $s<0$, equation (2.18) for $k\geq m+1$ reduces to

$$r(k)+\sum_{i=1}^{n} a_i r(k-i) \quad \text{if} \quad k>m \tag{2.19}$$

Equation (2. 19) is the basis for many estimators of the AR coefficients of AR (MA) processes.

AR Signals

In the ARMA class, the autoregressive or all-pole signals constitute the type that is most frequently used in applications. The AR equation may model spectra with narrow peaks by placing zeroes of the A-polynomial in the equation (2.9) with $B(\omega)\equiv 1$ close to the unit circle. In this study, using the Yule-Walker method to find the parameters and Based on the linear relationship between covariance and the parameters of AR.

Equation (2.19) for AR signals $m=0$ and $B(z)=1$ for $k>0$ Thus, the equation (2.18) that

$$r(0)+\sum_{i=1}^{n} a_i r(-i)=\sigma^2\sum_{j=0}^{m} b_j h_j^*=\sigma^2 \tag{2.20}$$

Combining equations (2.20) and (2.19) for $k=1,...,n$ giving the following system of linear equations

$$\begin{bmatrix} r(0) & r(-1) & \cdots & r(-n) \\ r(1) & r(0) & & \vdots \\ \vdots & & \ddots & r(-1) \\ r(n) & \cdots & & r(0) \end{bmatrix}\begin{bmatrix} 1 \\ a_1 \\ \vdots \\ a_n \end{bmatrix}=\begin{bmatrix} \sigma^2 \\ 0 \\ \vdots \\ 0 \end{bmatrix} \tag{2.21}$$

The above equations are called the Yule-Walker equation or Normal equations, and form the basis of many AR estimation methods. If $[r(k)], k = 0,...,n$ were known, could sole the equation (2.21) for

$$\theta = \left[a_1,...,a_n\right]^T \tag{2.22}$$

By using all but the first row of the equation (2.21):

$$\begin{bmatrix} r(1) \\ \vdots \\ r(n) \end{bmatrix} + \begin{bmatrix} r(0) & \cdots & r(-n+1) \\ \vdots & \ddots & \vdots \\ r(n-1) & \cdots & r(0) \end{bmatrix} \begin{bmatrix} a_1 \\ \vdots \\ a_n \end{bmatrix} = \begin{bmatrix} 0 \\ \vdots \\ 0 \end{bmatrix} \tag{2.23}$$

Or, with obvious definitions,

$$r_n + R_n\theta = 0 \tag{2.24}$$

The solution is $\theta = R_n^{-1} r_n$. Once θ is found, σ^2 can be obtained from the first row of the equation (2.21) or, equivalently, from the equation (2.20)

To explicitly stress the dependence of θ and σ^2 on the order n, can write the equation (2.21) as:

$$R_{n+1}\begin{bmatrix} 1 \\ \theta_n \end{bmatrix} = \begin{bmatrix} \sigma_n^2 \\ 0 \end{bmatrix} \tag{2.25}$$

MA Signal

According to the definition in the equation (2.15), an MA signal is obtained by filtering white noise with an all-zero filter. One method to estimate an MA spectrum consists of two steps:

1 Estimate the MA parameters $[b_k], k = 1,...,m$ and σ^2

2 Insert the estimated parameters from the first step in the MA PSD formula (see in the According to the definition in equation (2.9))

$$\varnothing(\omega) = \sigma^2 \left|B(\omega)\right|^2 \tag{2.26}$$

Another method to estimate an MA spectrum is based on the parameterization of the PSD in terms of the covariance sequence. See from equation (2.15) that for an MA of order m

$$r(k) = 0 \quad \text{for} \quad \left|k\right| > m \tag{2.27}$$

The definition of PSD and function of $r(k)$ turns into a finite-dimensional spectral model:

$$\varnothing(\omega) = \sum_{k=-m}^{m} r(k) e^{-j\omega k} \tag{2.28}$$

ARMA Signals

The modified Yule-Walker method is a two-stage procedure for estimating the ARMA spectral density. In the first stage the estimate the AR coefficients using equation (2.19). In the second stage, use the AR coefficients and ACS estimates in equation (2.8) to estimate the coefficients. The two steps was describe below:

Writing an equation (2.19) for $k = m+1, m+2, ..., m+M$ in a matrix form gives:

$$\begin{bmatrix} r(m) & r(m-1) & \cdots & r(m-n-1 \\ r(m+1) & r(m) & & r(m-n-1) \\ \vdots & & \ddots & \vdots \\ r(m+M-1) & \cdots & \cdots & r(m-n-M) \end{bmatrix} \begin{bmatrix} a_1 \\ \vdots \\ a_n \end{bmatrix} = - \begin{bmatrix} r(m+1) \\ r(m+2) \\ \vdots \\ r(m+M) \end{bmatrix} \tag{2.29}$$

If set $M = n$ in equation (2.29) obtain a system of n equations in the unknowns. This constitutes a generalization of the Yule-Walker system of equations that holds in the AR case. Replacing the theoretical covariance $r(k)$:

$$\begin{bmatrix} \hat{r}(m) & \cdots & \hat{r}(m-n+1) \\ \vdots & & \vdots \\ \hat{r}(m+n-1) & \cdots & \hat{r}(m-n+M) \end{bmatrix} \begin{bmatrix} \hat{a}(1) \\ \vdots \\ \hat{a}(n) \end{bmatrix} = - \begin{bmatrix} \hat{r}(m+1) \\ \vdots \\ \hat{r}(m+n) \end{bmatrix} \tag{2.30}$$

The above linear system can be solved for $(\hat{a}_i)$, which are called the modified Yule-Walker estimation of $(\hat{a}_i)$. The square matrix in equation (2.30).

CHAPTER 3
PHOTOPLETHYSMOGRAM SIGNAL

This chapter presents the basic aspects of the PPG technique. The basis for understanding the principle of PPG. A brief review of the early and recent history of PPG is included. Next, the PPG measurement system is described. Finally, PPG applications in clinical physiological measurements are presented.

3.1 Introduction

Photoplethysmography is an optical means to detect blood volume changes in the microvascular bed of tissue. Hertzman and Spielman [24] were the first to use the term 'photoplethysmography' and suggested that the resultant 'plethysmogram' represented volumetric changes in the blood vessels. PPG is most often employed noninvasively and operates at a red or a near infrared wavelength. The basic form of PPG technology requires only a few opto-electronic components: a light source to illuminate the tissue, and a photodetector to measure the small variations in light intensity associated with changes in blood perfusion. The most recognized waveform feature is the peripheral pulse, and it is synchronized to each heartbeat. Despite its simplicity the origins of the different components of the PPG signal are still not fully understood. It is generally accepted, however, that they can provide valuable information about the cardiovascular system. There has been a resurgence of interest in the technique in recent years, driven by the demand for low cost, simple and portable technology for the primary care and community based clinical settings, the wide availability of low cost and small semiconductor components, and the advancement of computer-based pulse wave analysis techniques. The PPG technology has been used in a wide range of commercially available medical devices for measuring oxygen saturation, blood pressure and cardiac output, assessing autonomic function and also detecting peripheral vascular diseases.

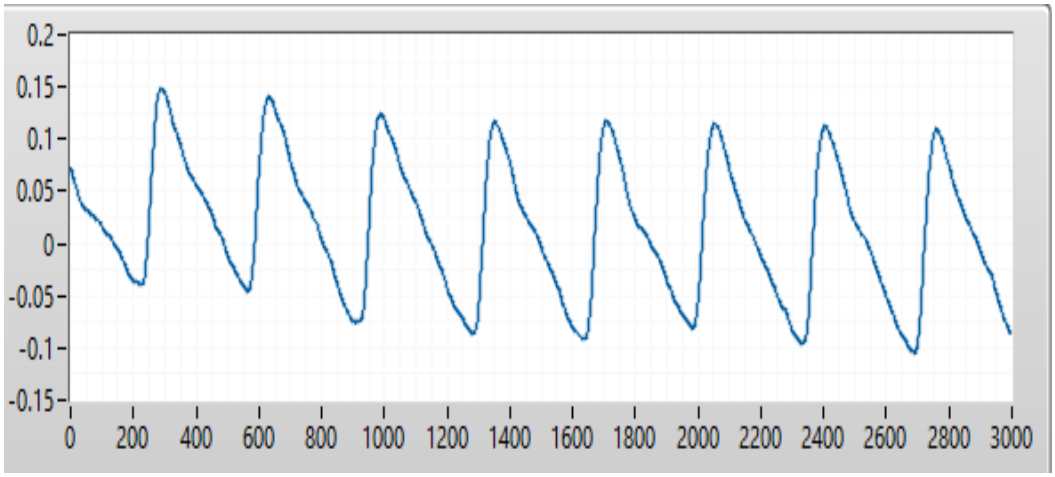

Figure 3.1 The example of photoplethysmogram signal

This section summarizes the early history of PPG and is taken from the important article. The first report of the application of PPG appeared, and described similar instrument used to monitor blood volume changes in the rabbit ear following venous occlusion and with administration of vasoactive drugs, Molitor and Kniazuk in 1936 [25] also described the satisfactory recordings obtained from the skin of the human fingers using a reflection mode PPG system. A great pioneer, to whom this method owes much of its success [26], who published his first paper on describing the use of a reflection mode system to measure blood volume changes in the fingers induced by exercise, cold and the Valsalva maneuver. His early work endeavored to establish the validity of the method for measuring blood flow and blood volume changes. And have split the AC and DC components with separate electronic amplifiers and monitored vasomotor activity [27]. In 1940, first used PPG for assessing the completeness of sympathectomy [28]. The early workers in this field were limited by the size, reproducibility and sensitivity of their photodetectors. The advance of semiconductor technology these detectors has become much smaller and more sensitive and later authors have been able to investigate the technique were developed. Have used PPG to detect the onset of cutaneous vasodilatation in both forearm and digits. Many authors have applied PPG to tubed pedicles. More recently, advances in opto-electronics and clinical instrumentation have significantly contributed to PPG's advancement. A major advance in the clinical use of a PPG-based technology came with the introduction of the pulse oximeter as a noninvasive method for monitoring patient's arterial oxygen saturation [29].

PPG has been applied in many different clinical settings, including the monitoring of blood oxygen saturation, heart rate, blood pressure, cardiac output and respiration [30]. Given its simplicity, low-cost and that it is widely used in the clinical routine, it is generally accepted that PPG can provide valuable information about the cardiovascular system. The autonomic influences on the PPG signal have been analyzed in several studies, and recently, pulse rate variability extracted from PPG has been studied as a potential surrogate of heart rate variability [31-34]. The HRV analysis is one of the most widely used non-invasive techniques for the evaluation of the autonomic nervous system. The use of PRV as a surrogate of HRV could be useful in applications where the ECG is not available, or when it is beset with electrical artifacts [35]. Moreover, since PPG also allows us to derive physiological parameters such as blood oxygenation and ventilatory rate, the use of PRV instead of HRV could be particularly suitable in those applications where the simultaneous acquisition of many signals is required, as for example in sleep disorder studies, mainly for ambulatory sleep studies. The main difference between HRV and PRV is the time the pulse wave takes to travel from the heart of the finger. This time is called the pulse transit time (PTT) and is typically measured as the difference between the peak of the R-wave on the ECG and the peak value of the corresponding pulse in the finger pad measured by PPG. PTT, which is tie-related to arterial compliance and blood pressure, changes beat to beat [36-38]. Thus, the PRV is also affected by the variability in the PTT, i.e. the beat-to-beat changes in the pulse wave velocity.

The oscillations of cardiovascular parameters are widely used for evaluating the regulation between autonomic nervous system and cardiovascular system, and are expected to provide information for the prediction and prevention of cardiovascular disease [3]. An example widely used is the Item rate variability. It is usually insured by spectral analysis of the R-R interval from ECG signal. The Low frequency component of HRV reflects the sympathetic activities of ANS while the high frequency component reflects the palm sympathetic (vagal) activities. Which are corresponding to the respiratory rhythm [22]. A heartbeat will generate a corresponding PPG pulse at peripheral position. Compared to ECG monitoring which needs to attach several electrodes on the body. PPG monitoring at peripheral position is much more convenient. The sensors can be embedded in the phone camera, ring, glass, chair or bed sheet for unobtrusive measurement. Therefore. PPG was proposed as a surrogate of ECG for the analysis of HRV [21] and [39-41]. A comparison between different features of the HRV

signals derived from both methods was performed to test the validity of using PPG signals in HRV analysis [42].

All the studies exploring the possibility of using Pulse rate variability as an alternative measure of HRV have been performed in stationary conditions using time domain, frequency domain analysis and generally showed that PRV is a good surrogate of HRV [43]. However, there are many situations where significant changes in autonomic balance occur, as during exercise test, which involve non-stationary processes. In such situations, the use of PRV as an alternative measurement of HRV could be of great interest.

3.2 The Photoplethysmogram Waveform

The principle of PPG has been reviewed previously [44], and is explained briefly here. Light travelling though biological tissue can be absorbed by different substances, including pigments in the skin, bone, and arterial and venous blood. Most changes in blood flow occur mainly in the arteries and arterioles (but not in the veins). For example, arteries contain more blood volume during the systolic phase of the cardiac cycle than during the diastolic phase. PPG sensors optically detect changes in the blood flow volume (i.e., changes in the detected light intensity) in the microvascular bed of tissue via reflection from or transmission through the tissue. Figure 3.1 shows an example of a photoplethysmogram waveform, consisting of direct current and alternating current components. The DC component of the PPG waveform corresponds to the detected transmitted or reflected optical signal from the tissue, and depends on the structure of the tissue and the average blood volume of both arterial and venous blood. Note that the DC component changes slowly with respiration. The AC component shows changes in the blood volume that occurs between the systolic and diastolic phases of the cardiac cycle; the fundamental frequency of the AC component depends on the heart rate and is superimposed onto the DC component.

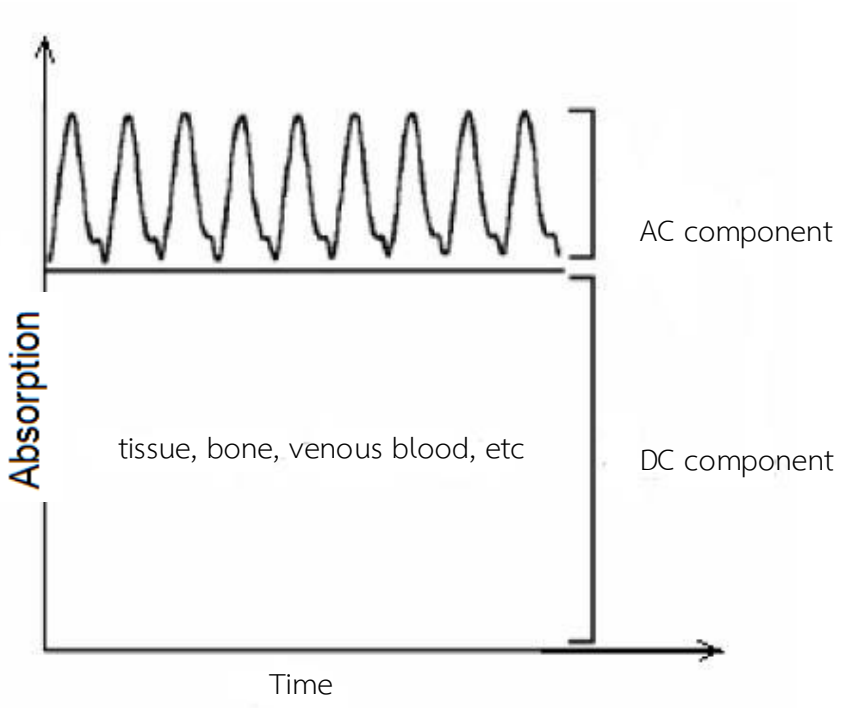

Figure 3.2 Typical PPG waveform showing the 'AC' and 'DC' components

Photoplethysmography measurement system, most of PPG instruments consist of an optoelectronic sensor that is applied to the patient and a microproce-ssorbased system that processes and displays the measurement. The optoelectronic sensor usually contains the low-voltage, high-intensity light-emitting diodes (LED) as light sources to shine light onto an area of tissue and one photodiode as a light receiver to convert an optical signal into an electrical signal. The light from the LED is transmitted through the tissue at the sensor site. A portion of light is absorbed by skin, tissue, bone, and blood. The photodiode, in response to the optical signal from the LED, measures the transmitted light.

Two modes of measurement are generally used, namely the transmission" and "reflection" modes, depending on the relative positions of the emitter and detector as shown in Figure 3.3

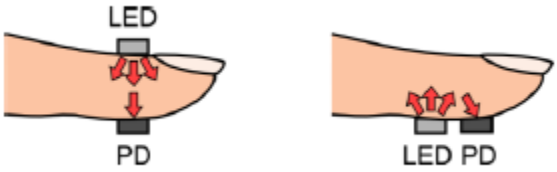

Figure 3.3 Light-emitting diode (LED) and photodetector (PD) placement for transmission and reflectance-mode photoplethysmography.

For our study the participant was equipped with an optical transducer for recording the PPG at the fingertip. All sensors were connected to an Analog-to-Digital Converter unit (MP36 Biopac Systems Inc., Santa Barbara, CA, USA). Data were displayed and stored at 500Hz sampling frequency in the computer for the off-line analysis (Figure 3.4).

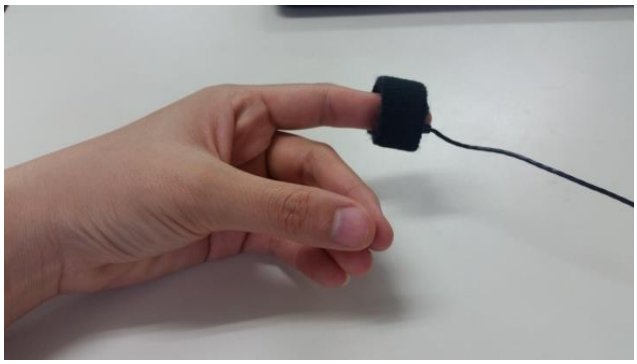

Figure 3.4 The example of Finger photoplethysmogram transducer

3.3 Photoplethysmography Applications in Clinical Physicolo-gical measurement

PPG has been applied in many different clinical settings, such as clinical physiological monitoring, vascular assessment, and autonomic function, etc. Pulse oximetry has been one of the most significant technological advances in clinical patient monitoring over the last few decades. It utilizes PPG measurements to obtain information about the arterial blood oxygen saturation (SpO2) and heart rate. Some of the main areas in which they are used include anesthesia, patient transport, fetal monitoring, neonatal and pediatric care, dentistry and oral surgery, and sleep studies. The pulse oximetry became a mandated international standard for monitoring during anesthesia. A recent and

exciting development in pulse oximetry is the noninvasive measurement of venous oxygen saturation using external artificial perturbations applied close to the PPG probe.

Respiration causes variation in the peripheral circulation, making it possible to monitor breathing using a PPG sensor attached to the skin. The low frequency respiratory induced intensity variations in the PPG signal are well documented. The stroke volume (the amount of blood pumped out of a ventricle during one ventricular contraction) can be estimated from PPG-derived pulse contour analysis on a beat-by-beat basis. However, there is ongoing discussion in the literature with regard to the accuracy of PPG-based cardiac output assessments.

CHAPTER 4
EXPERIMENTAL SYSTEM

This chapter introduces the experiment protocol, methodology of Heart Rate Variability analysis, a statistical method for cross correlation between two signals in resting and exercises conditions. The stages of the research are as the following diagram:

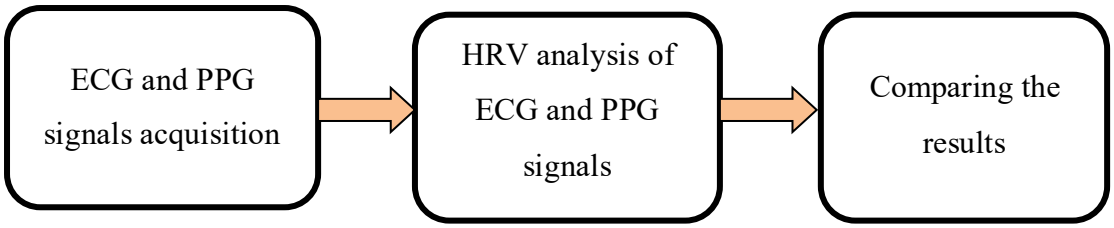

Figure 4.1 Block diagram of ECG and PPG signals for HRV analysis

4.1 Experiment Protocol and ECG, PPG Signals Recording

Thirty three biomedical engineering students (20 males and 13 females) participated in this study. Their demographics (mean±SD) are presented in Table 4.1

Table 4.1 Demographics of participants

No. of Participants	Age (year)	Height (cm)	Weight (kg)
33	21.34±1.42	168.28±8.05	67.87±12.6

The young and healthy subjects participated in the experiments. At the beginning of test, each participant was equipped with an optical transducer for recording the PPG at the fingertip and three surface electrodes were placed on the body for ECG (lead II) monitoring [11]. All sensors were connected to an Analog-to-Digital Converter unit (MP36 Biopac Systems Inc., Santa Barbara, CA, USA). Data were displayed and stored at 500Hz sampling frequency in the computer for the off-line analysis. The experiment is divided into two parts, resting and an exercise. Participants were first asked to lie down with eyes closed in a quiet room for 10 minutes. They were, in the next 15 minutes, doing exercise on a stationary bicycle to increase their HR to higher than 130 beats/minute continuously for at least 5 minutes as show in Figure 4.2

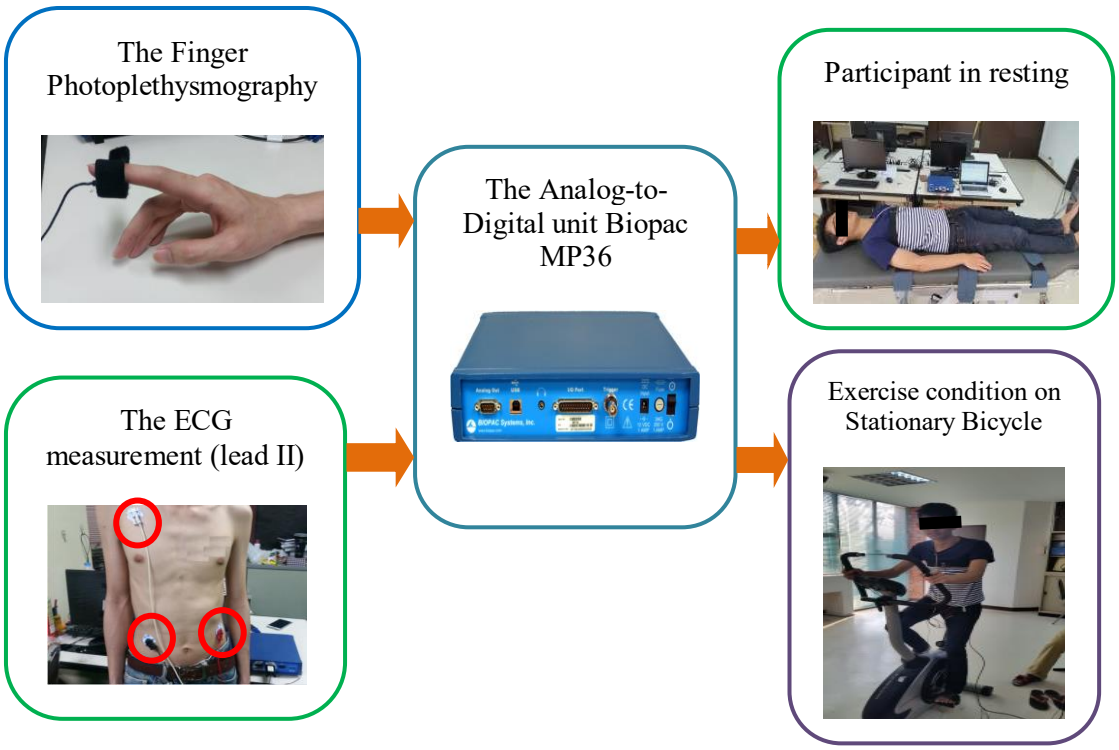

Figure 4.2 ECG and PPG data measurement process use Bio-pac system

For each trial, the two 5-minute portion of PPG and ECG were selected from resting and exercise conditions as demonstrated in Figure 4.3 for analysis.

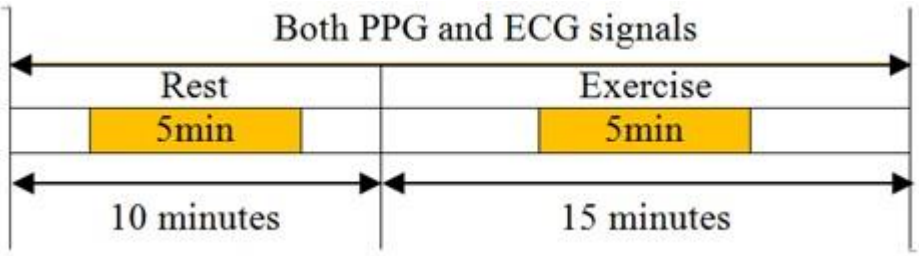

Figure 4.3 Selected 5-minute portions from both conditions

4.2 Analysis of HRV from ECG and PPG signals

Heart Rate Variability is well known to be the measure of cardiac autonomic function. The two branches of systemic control, sympathetic and parasympathetic (vagal) modulations, are reflected in the variation of heart beat interval in Electrocardiogram [3]. HRV has been used in a large number of research to study physiological and

psychological dysfunctions. Though it gains popularity as the noninvasive marker, the setup of ECG recording is sometimes inconvenient, particularly in study with movement activities.

Photoplethysmography is a simple and widely used technique for measuring changes in blood volume. The finger photoplethysmography is often found anywhere in form of a portable standalone unit or part of the sophisticated bedside monitor system. In clinic, the primary function of PPG device is to monitor arterial oxygen saturation (SaO_2). PPG signal also provides valuable information of cardiac autonomic activity via the pulsatile waveform. The samples of simultaneously recorded ECG and PPG are given in Figure 4.4

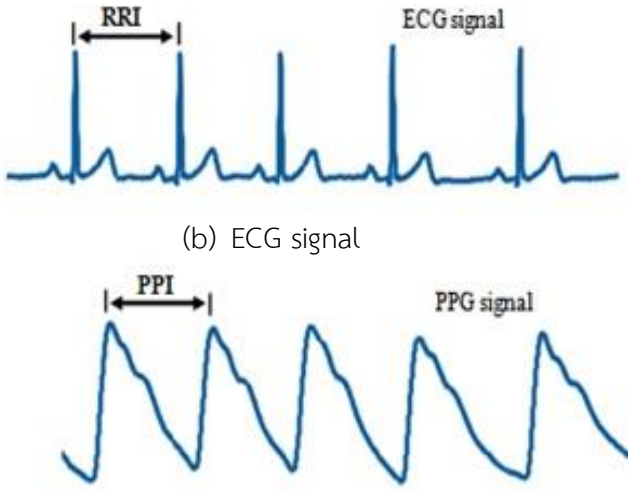

Figure 4.4 The example signals of (a) ECG signal and (b) PPG signal

Photoplethysmography has been considered as a promising surrogate for ECG in measuring heart rate variability. The High correlation between pulse intervals and RR intervals were obtained in some studies, and it was concluded that pulse variability can serve as an alternative approach to obtain HRV information [6], [21] and 43]. However, there stood only resting condition. So in our work we use the rest and exercise condition for this research, to study the HRV from PP Intervals of PPG and RR intervals of ECG signals. In this research, the beat-to-beat interval waveforms extracted from PPG and ECG were generated as show in Figure 4.5

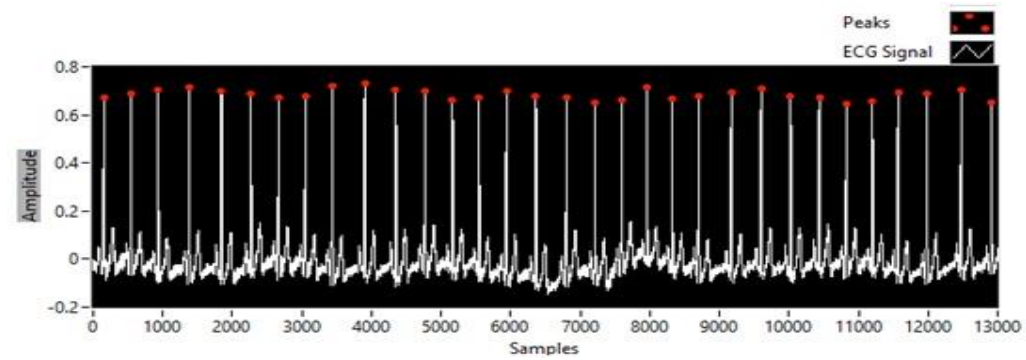

(a)

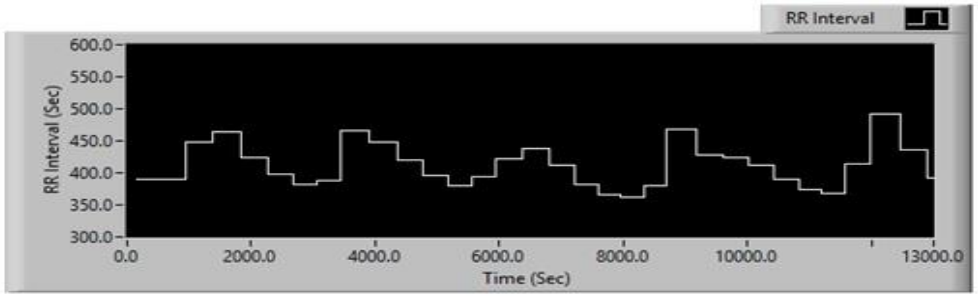

(b)

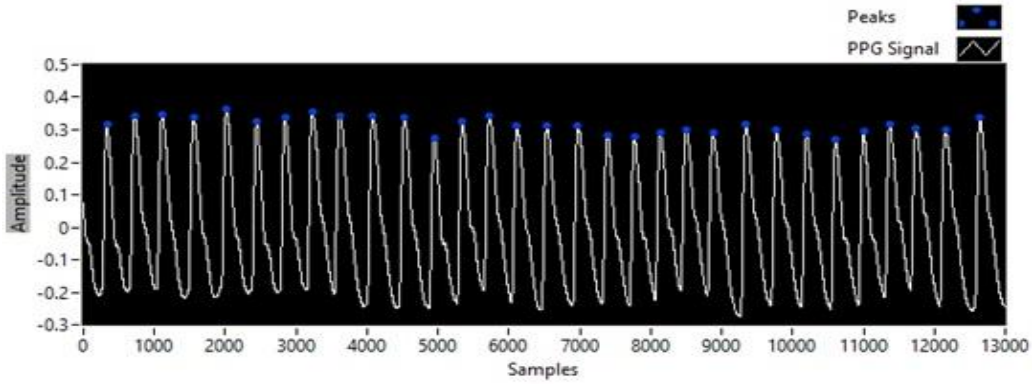

(c)

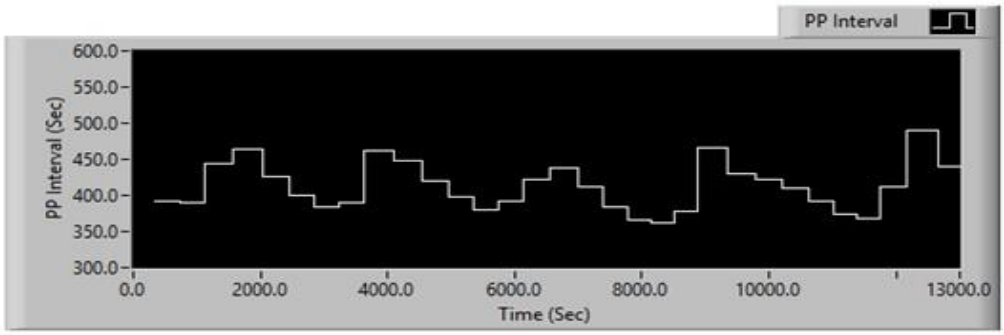

(d)

Figure 4.5 (a) Example of ECG signal, (b) RRI signal derived from ECG, (c) Sample of PPG signal, (d) PPI signal derived from PPG.

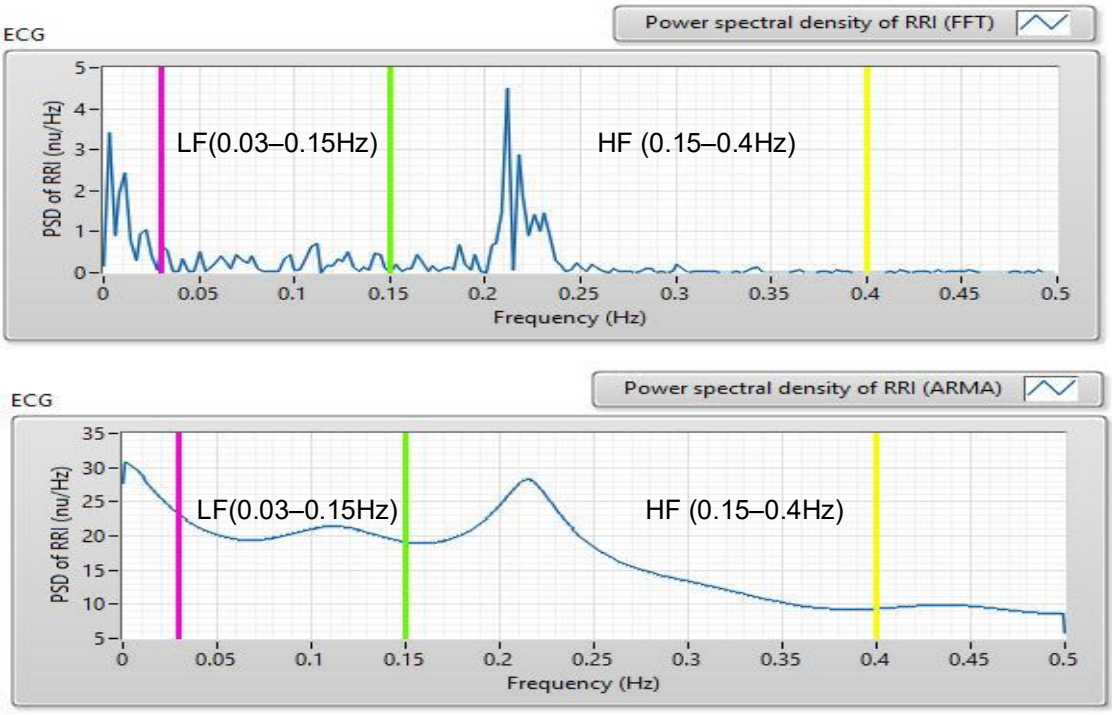

(a) Power spectral density of RR interval derives from ECG

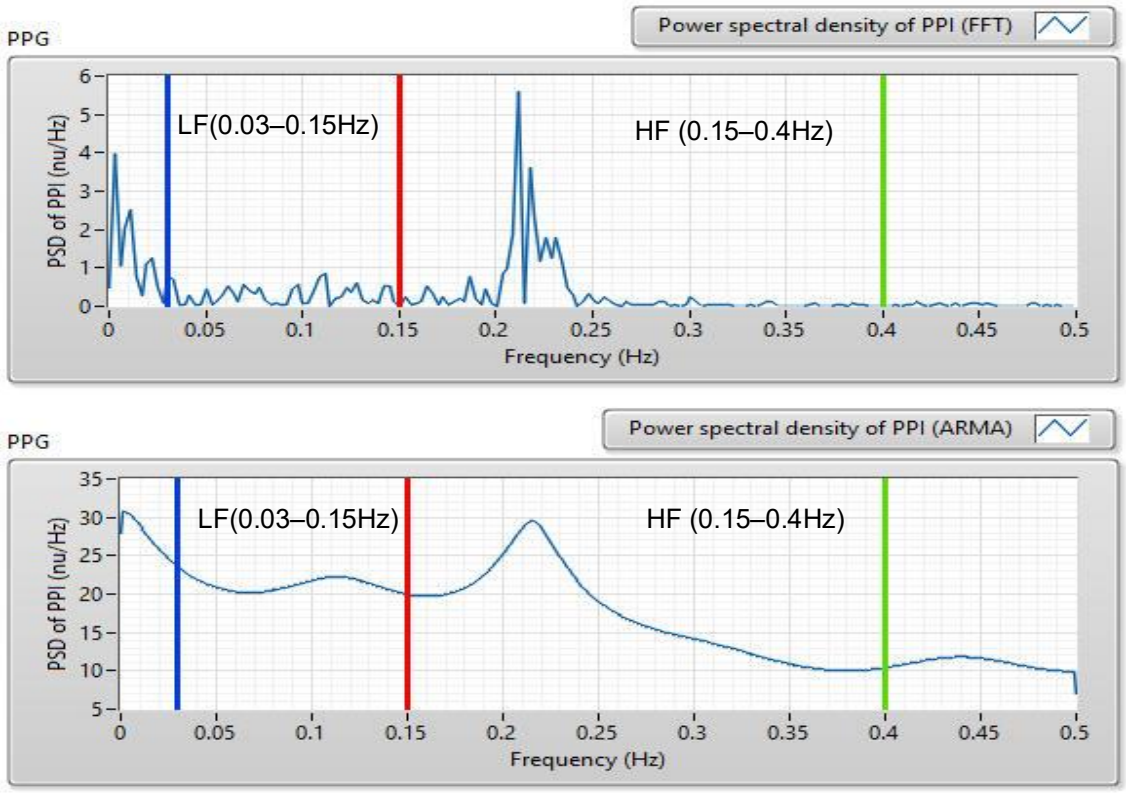

(b) Power spectral density of PP interval derives from PPG

Figure 4.6 (a, b) Selected frequency domain measures of HRV

The cross correlation between two waveforms were evaluated during resting and exercise using time domain and frequency domain methods. In addition, we computed two statistical parameters, mean and standard deviation, of heart rate based on those waveforms. They are two fundamental parameters for computing HRV indices. Finally, both parameters were compared by regression analysis

4.3 The technique for comparing statistics

4.3.1 Correlation Coefficient

The quantity r, called the linear correlation coefficient, measures the strength and the direction of a linear relationship between two variables. The linear correlation coefficient is sometimes referred to as the Pearson product moment correlation coefficient in honor of its developer Karl Pearson.

- The value of r is such that $-1 \leq r \leq +1$. The + and – signs are used for positive linear correlations and negative linear correlations, respectively.
- Positive correlation: If x and y have a strong positive linear correlation, r is close to +1. An r value of exactly +1 indicates a perfect positive fit. Positive values indicate a relationship between x and y variables such that as values for x increases, values for y also increase.
- Negative correlation: If x and y have a strong negative linear correlation, r is close to -1. An r value of exactly -1 indicates a perfect negative fit. Negative values indicate a relationship between x and y such that as values for x increase, values for y decrease.
- No correlation: If there is no linear correlation or a weak linear correlation, r is close to 0. A value near zero means that there is a random, nonlinear relationship between the two variables.
- Note that r is a dimensionless quantity; that is, it does not depend on the units employed.
- A perfect correlation of ± 1 occurs only when the data points all lie exactly on a straight line. If r = +1, the slope of this line is positive. If r = -1, the slope of this line is negative.

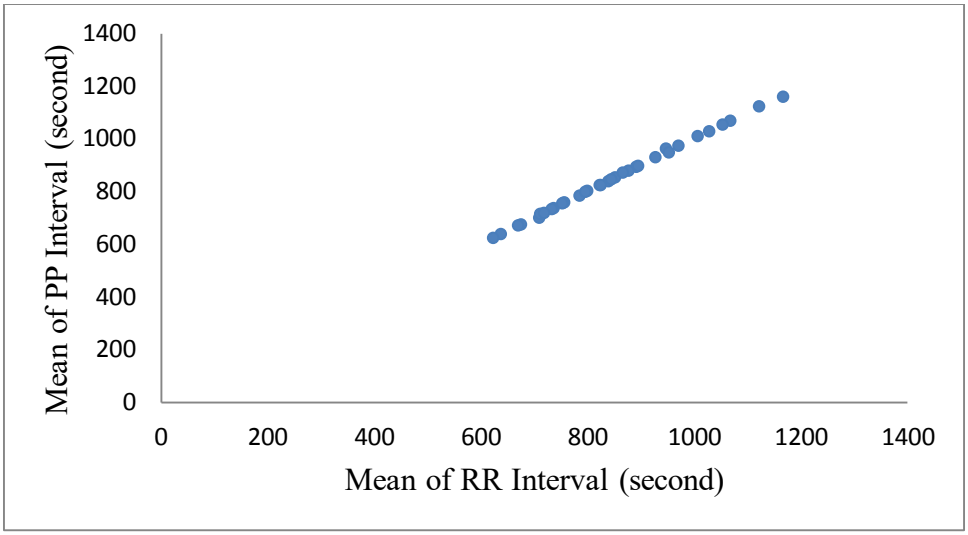

(a)

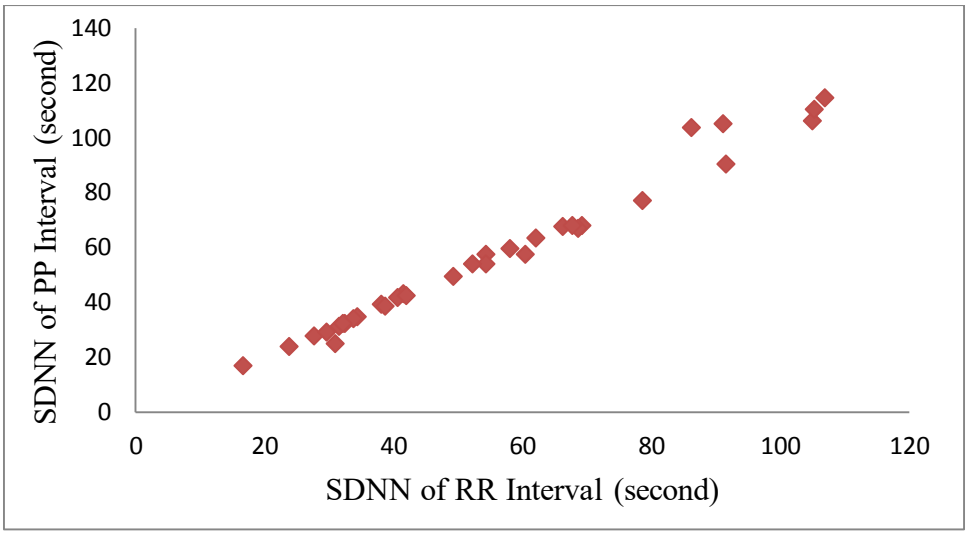

(b)

Figure 4.7 (a, b) The two scatter plot graphs on the top represent an example of data correlation coefficients between Mean, SDNN of RRI and PPI in resting condition. The graphs demonstrate a positive correlation coefficient.

4.3.2 Coefficient of Determination

The coefficient of determination, R^2, is useful because it gives the proportion of the variance (fluctuation) of one variable that is predictable from the other variable. It is a measure that allows us to determine how certain one can be in making predictions from a certain model/graph:

- The coefficient of determination is the ratio of the explained variation to the total variation.

- The coefficient of determination is such that $0 \leq R^2 \leq 1$, and denotes the strength of the linear association between x and y.
- The coefficient of determination represents the percent of the data that is the closest the line of best fit.
- The coefficient of determination is a measure of how well the regression line represents the data. If the regression line passes exactly through every point on the scatter plot, it would be able to explain all of the variation.

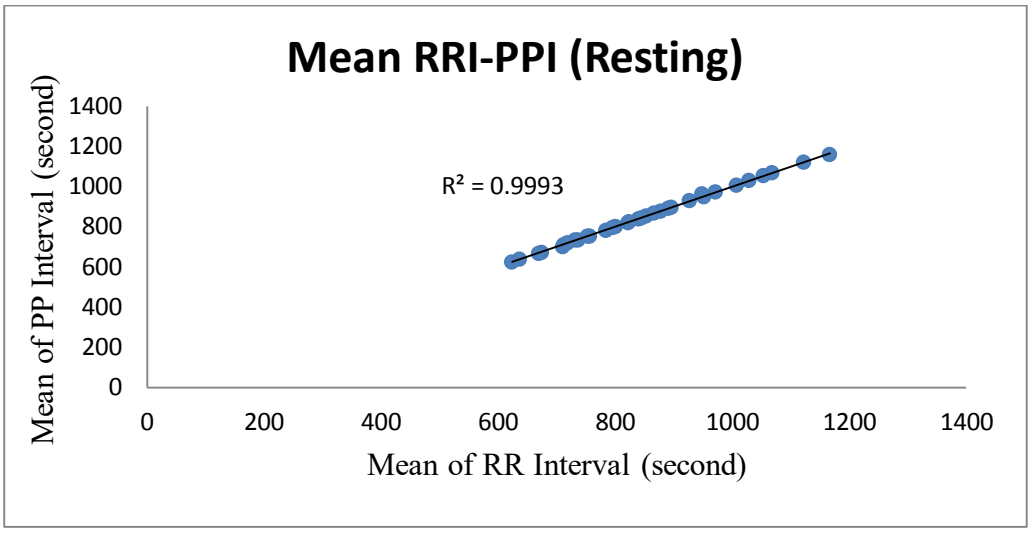

(a)

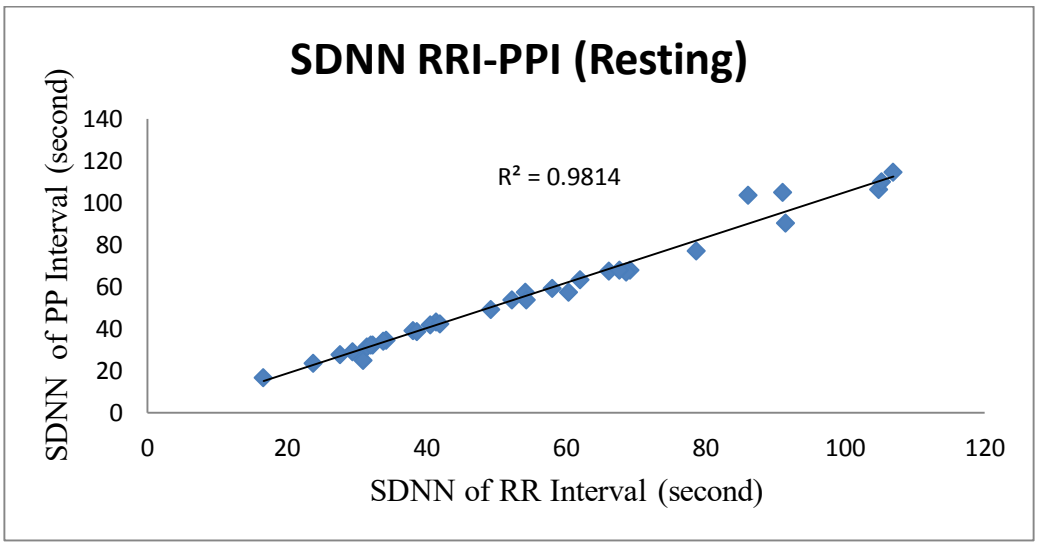

(b)

Figure 4.8 (a, b) The determination coefficient, R^2, regression analysis (a). between two means in resting state, (b). between two SDNNs in resting state.

CHAPTER 5
EXPERIMENTAL RESULTS

This thesis is to investigate the possibility of computing Heart Rate Variability (HRV) indices from the finger Photoplethysmogram. To indicate that whether Peak to Peak interval from PPG signal can be used as an alternative to Heart Rate Variability from the ECG signal from 33 participants in both resting and exercise conditions all of 5 minutes.

5.1 Heart Rate Variability Analysis Extracts from ECG and PPG Signals in Resting Condition

The result from heart rate variability analysis are divided into time-domain, frequency-domain results both the ECG and PPS signals from 33 participants in resting conditions all of 5 minutes. Time-domain HRV measures considered included mean RR, SDNN. Peak LF and Peak HF in absolute and normalized units were considered for frequency-domain analysis.

5.1.1 Time domain method

- The time-domain results from HRV analysis of MeanRR in resting condition

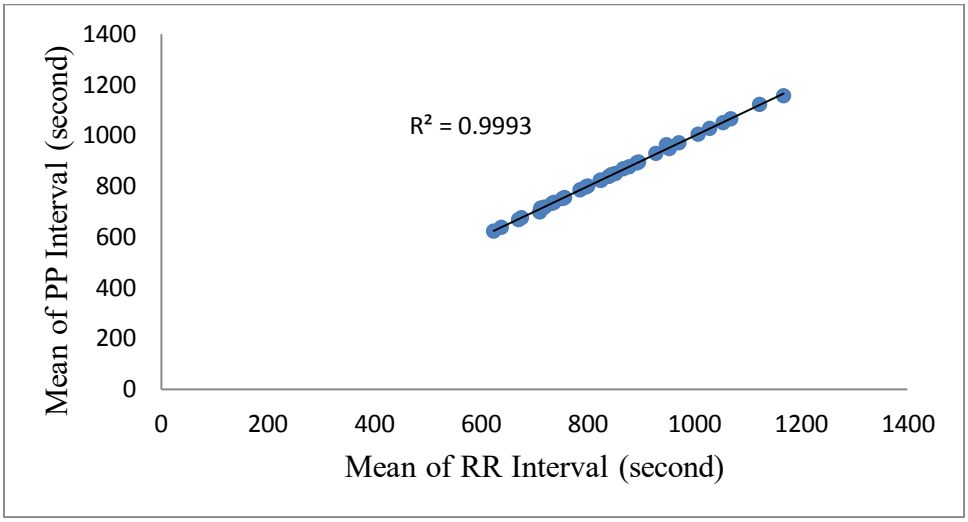

Figure 5.1 The time-domain results from HRV analysis of MeanRR all of the subject in resting condition derived from ECG and PPG signals

- The time-domain results from HRV analysis of SDNN in resting condition

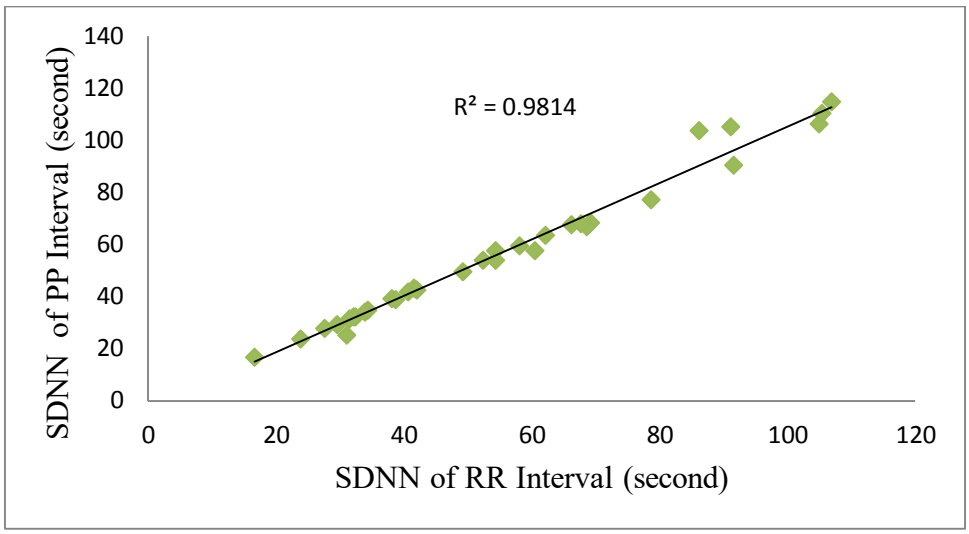

Figure 5.2 The time-domain results from HRV analysis of SDNN all of the subject in resting condition derived from ECG and PPG signals

5.1.2 Frequency Domain Method

- The frequency domain results from HRV analysis of LF in resting condition

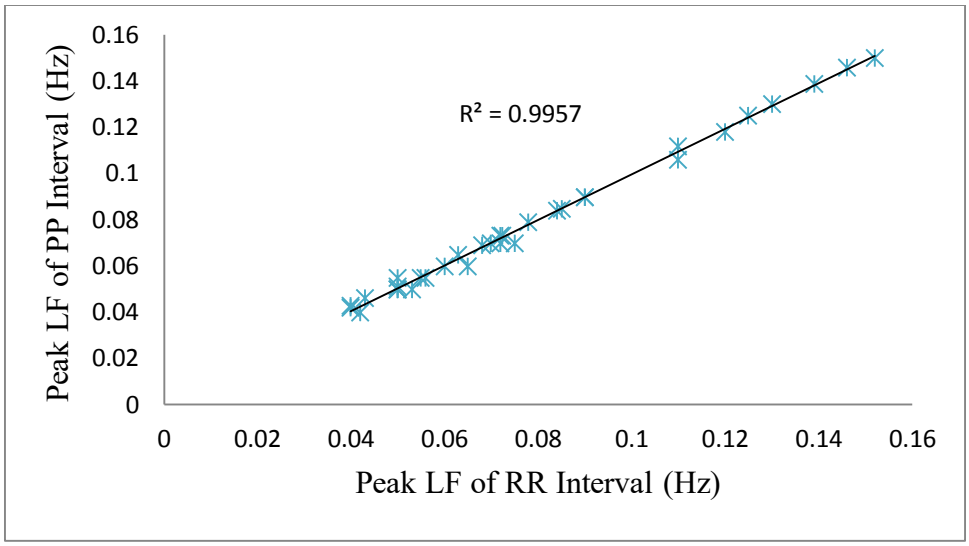

Figure 5.3 The frequency domain results from HRV analysis of LF all of the subject in resting condition derived from ECG and PPG signals.

- The frequency domain results from HRV analysis of HF in resting condition

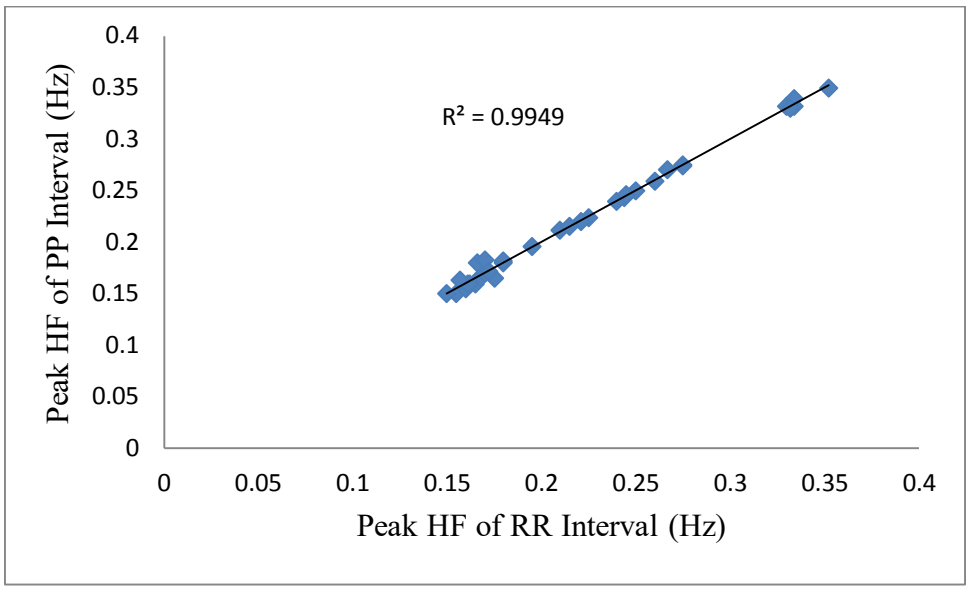

Figure 5.4 The frequency domain results from HRV analysis of LF all of the subject in resting condition derived from ECG and PPG signals

5.2 Heart Rate Variability Analysis Extracts from ECG and PPG Signals in Exercise Condition

The result from heart rate variability analysis are divided into time-domain, frequency-domain results both the ECG and PPS signals from 33 participants in exercise conditions all of 5 minutes. Time-domain HRV measures considered included mean RR, SDNN. LF and HF power in absolute and normalized units were considered for frequency-domain analysis.

5.2.1 Time Domain Method

- The time-domain results from HRV analysis of Mean RR in exercise condition

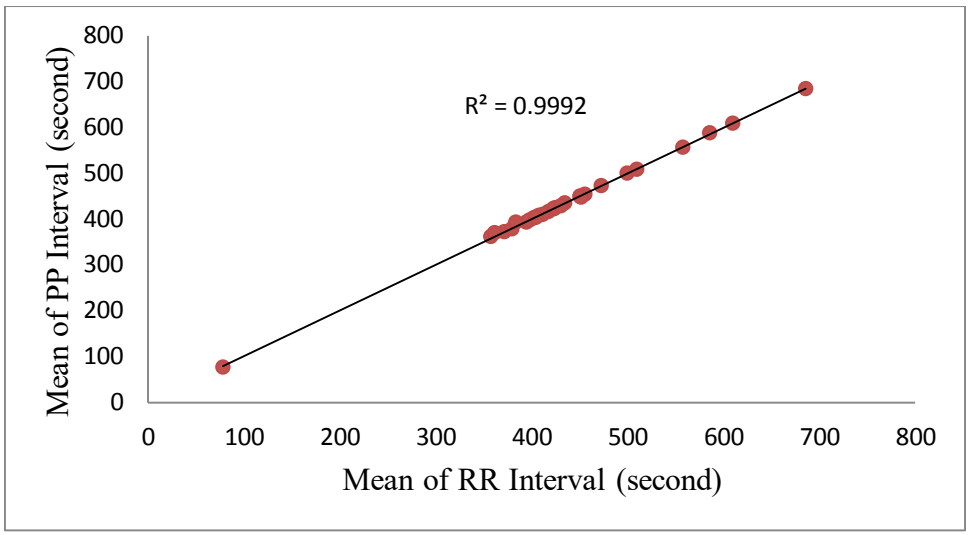

Figure 5.5 The time-domain results from HRV analysis of MeanRR all of the subject during an exercise condition derived from ECG and PPG signals

- The time-domain results from HRV analysis of SDNN in exercise condition

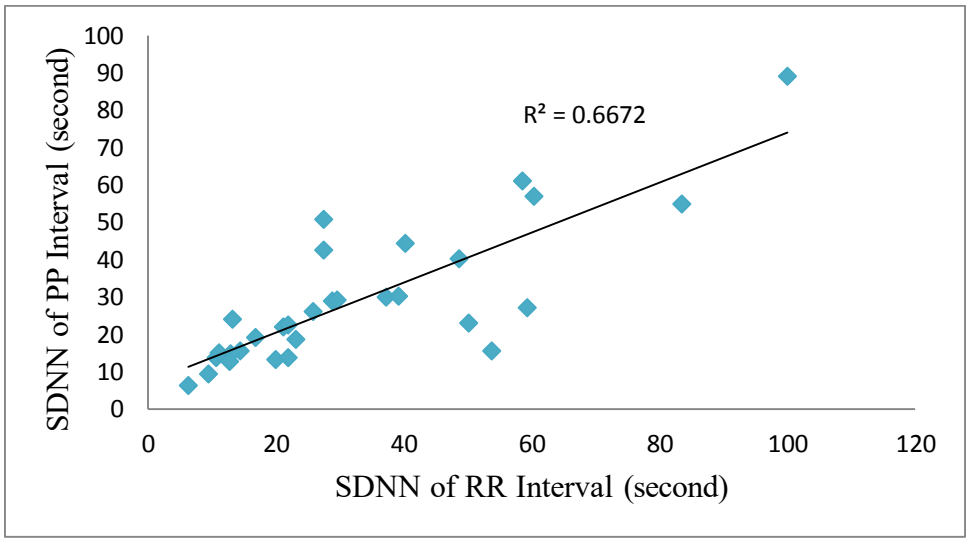

Figure 5.6 The time-domain results from HRV analysis of SDNN all of the subject during an exercise condition derived from ECG and PPG signals

5.2.2 Frequency Domain Method

- The frequency domain results from HRV analysis of LF in exercise condition

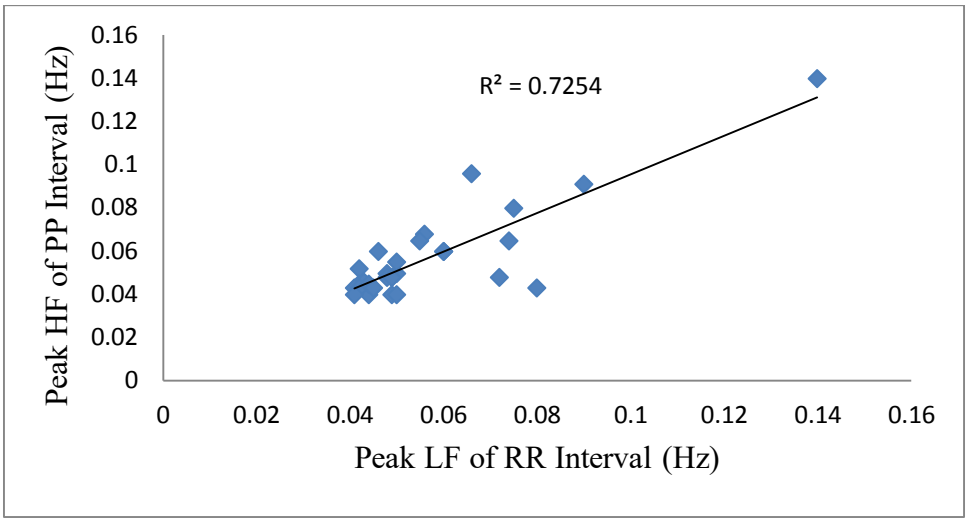

Figure 5.7 The frequency domain results from HRV analysis of LF all of the subject on the exercise condition derived from ECG and PPG signals

- The frequency domain results from HRV analysis of HF in exercise condition

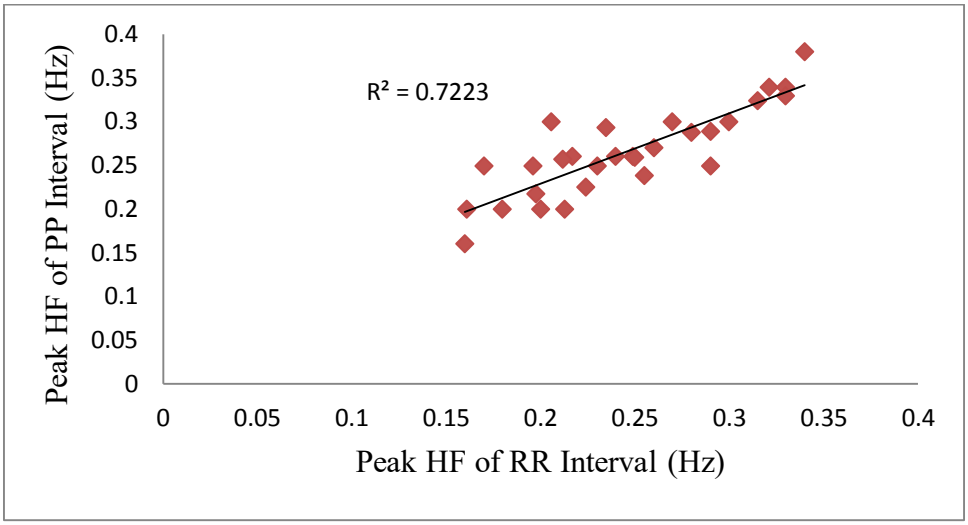

Figure 5.8 The frequency domain results from HRV analysis of HF all of the subject on the exercise condition derived from ECG and PPG signals

5.3 Comparison Heart Rate Variability from ECG with PPG in Resting and Exercise condition

The feasibility of the PPG variability was verified by correlation coefficient, which all demonstrated high correlation between the two signals. We observed that the PPG signal obtained during the resting condition has more cognate than during the exercise condition, as evidenced by a lower correlation between the HRV extract from ECG and PPG signals as shown in Figure 5.8 and 5.9. The current work strongly suggests a good alternative to understanding dynamics pertaining to the autonomic nervous system without the use of an ECG device.

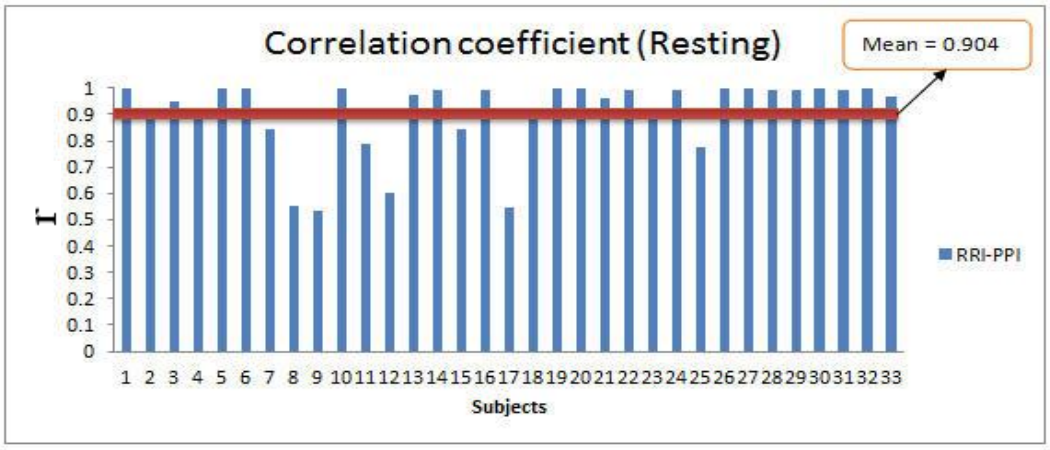

Figure 5.9 The correlation coefficients, r, between the RRI and PPI during resting state (n=33, the average 'r' is 0.904)

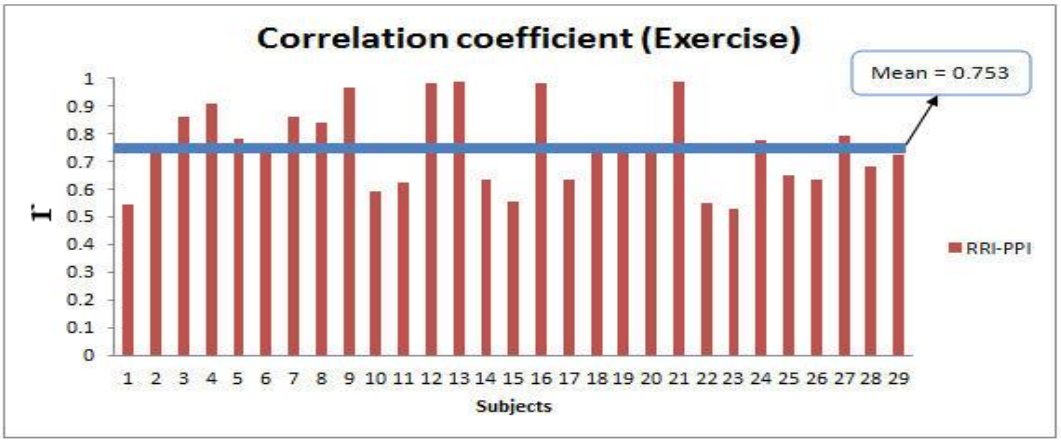

Figure 5.10 The correlation coefficients, r, between the RRI and PPI during exercise (n=29, the average 'r' is 0.753)

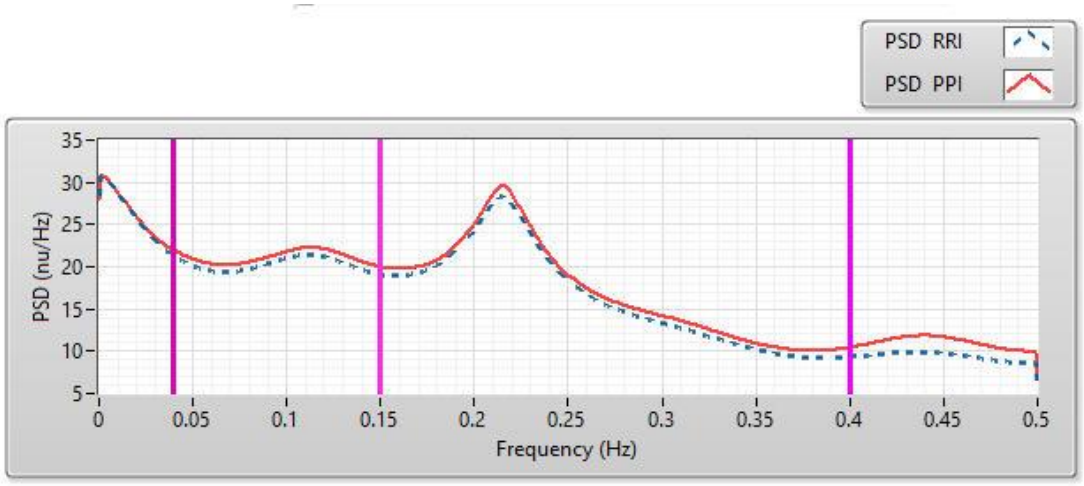

Figure 5.11 Comparison power spectrum density of HRV between two signals during resting

5.4 Comparison Heart Rate Variability in Resting and Exercise condition

The average value of r calculated from the cross correlation between PPI and RRI suggests that these two beat-to-beat interval time series are consistent with higher degree in resting than exercise. Supported by the evidence of R^2 from regression analysis of statistical parameters in Table 5.1, the bigger numbers (R^2 of mean and SDNN) are reported in resting. All lower indicators in exercise are due to the quality of acquired signals. And In rest condition the result has the close value with other research from the correlation coefficient and the coefficient of determination calculated. So the PP intervals from PPG signal can be used as an alternative to heart rate variability from the ECG signal in both the rest and exercise condition. However, during the exercise condition depends on the applications.

Table 5.1 Determination coefficients (R^2) of Mean, SDNN, LF and HF, between Resting and Exercise condition

Condition	Mean	SDNN	Peak of LF	Peak of HF
Resting	0.9993	0.9814	0.9957	0.9949
Exercise	0.9987	0.6651	0.7254	0.7223

Usually, the fluid dynamic of blood circulation, cardiac arrhythmia and blood vessel's compliance play a key role in PPG fluctuation. The movement artifact, however, can seriously contaminate both PPG and ECG during exercise. Figure 5.12 and 5.13 demonstrate examples of the ECG and PPG during exercise with undetected peaks. These irregular patterns make difficulty to correctly find the peaks and lead to erroneous beat-to-beat waveform formation.

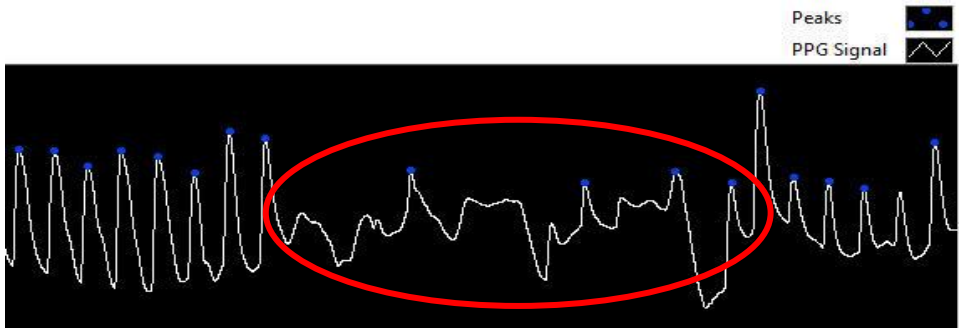

Figure 5.12 Example of contaminated PPG during exercise

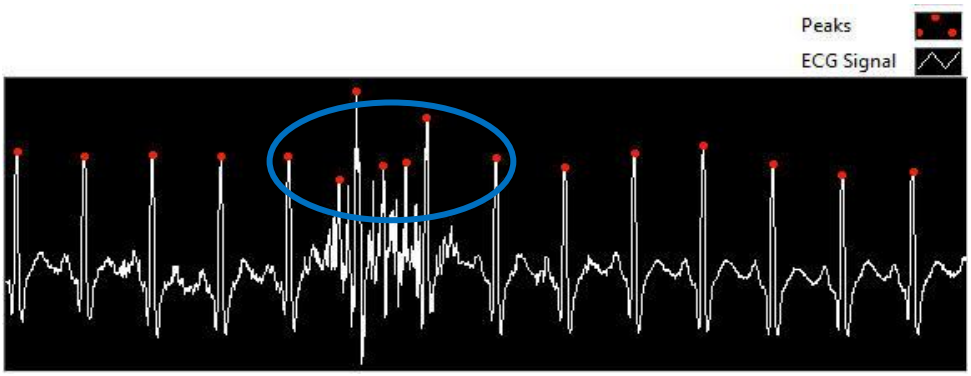

Figure 5.13 Example of contaminated ECG during exercise

CHAPTER 6
CONCLUSIONS AND DISCUSSION

6.1 Conclusions and Discussion

This thesis is to investigate the possibility of computing Heart Rate Variability indices from the finger Photoplethysmogram. To indicate that whether Peak to Peak interval from PPG signal can be used as an alternative to heart rate variability from the ECG signal from 33 participants in both resting and exercise conditions all of 5 minutes.

The average value of r calculated from the cross correlation between PPI and RRI suggests that these two beat-to-beat interval time series are consistent with higher degree in resting than exercise. Supported by the evidence of R^2 from regression analysis of statistical parameters (R^2 = 0.981), the bigger numbers (R^2 of mean and SDNN) are reported in resting, which in the exercise (R^2 = 0.665). All lower indicators in exercise are due to the quality of acquired signals. And In rest condition the result has the close value with other research from the correlation coefficient and the coefficient of determination calculates. And the PP intervals from PPG signal can be used as an alternative to heart rate variability from the ECG signal in both the rest and exercise condition. However, during the exercise condition depends on the applications.

Normally, the fluid dynamic of blood circulation, cardiac arrhythmia and blood vessel's compliance play a key role in PPG fluctuation. The movement artifact, however, can seriously contaminate both PPG and ECG during exercise. Figure 5.12 and 5.13 in chapter 5 are demonstrating samples of the ECG and PPG during exercise with undetected peaks. These irregular patterns make difficulty to correctly find the peaks and lead to erroneous beat-to-beat waveform formation.

Physiologically, ECG and PPG are both originated from the cardiovascular system. They are in fact generated from different mechanisms. Cardiac pacemaker is electrically monitored by ECG while the PPG is the result of mechanical wave (blood pressure) travelling from the left ventricle to the finger. Their variability of HR are expectedly identical.

Our study concludes that HRV indices can be calculated with confidence from PPG during the resting state. The inconsistent value, R^2 of mean and SDNN, Peak LF and Peak HF during exercise is the consequence of poor PPG and ECG signals quality causing incorrect peak detection. An alternative technique to better identify the beat-to-

beat interval is needed. The study showed valley-to-valley interval of PPG gives higher accuracy than the peak-to-peak detection. This will be part of our development.

An interest in wearable technology brings an attention to PPG. To assess long term HRV analysis, PPG's beat intervals gain more attraction than ECG's counterparts. As a compact, non-invasive, multipurpose device, finger plethysmographaphy is future health care self-monitoring solution.

REFERENCES

[1] P. Muaynoi, S. Tretriluxana, and K. Chitsakul, "The effect of exercise on heart rate variability analysis case study: stress in Rat," *Master Thesis of King Mongkut's Institute of Technology Ladkrabang,* 2013.

[2] A. Punapung, S. Tretriluxana, and K. Chitsakul , "A standard 12lead electrocardiogram with wireless network capability," *Master Thesis of King Mongkut's Institute of Technology Ladkrabang*, 2012.

[3] "Task force of the European society of cardiology and the North American Society of Pacing and electophysiology. Haeart rate variability: Stand of measurement physiological interpretation, and clinical use," *American Heart Association, European Society of Cardiology Standards of heart rate variability,* pp. 354-381, March 1996.

[4] N. Salome, S. Ngampramuan and N. Nalivako, "Intra-Amygdala Injection of Gabaa Agonist, Muscimol, Reduces Tachycardia and Modifies Cardiac Sympatho-Vagal Balanch during Restraint Stress in Rats," *American Journal of Physiology-Regulatory, Integrative and Comparative Physiology*, *Neuroscience* 148, pp. 335-341, 2007.

[5] W. Wanqing and L. Jungtae, "Development of Full-Featured ECG System for Visual Stress Induced Heart Rate Variability (HRV) Assessment," *In proceeding of Signal Processing and Information Technology (ISSPIT), IEEE International Symposium on,* pp. 144-149, 2010.

[6] B. Golosarsky, "Can heart rate variability timing reflect the body stress?," *International Journal of Cardiology, Hypotheses*, pp. 1467-1468, 2006.

[7] EH. Hon and ST. Lee, "Electronic evaluation of the fetal heart rate patterns preceding fetal death," *American Journal of Obstetrics & Gynecology*, Vol. 87, pp. 814-826, 1965.

[8] MM. Wolf, GA. Varigos, D. Hunt and JG. Sloman, "Sinus arrhythmia in acute myocardial infarction," *Medical Journal of Australia*, Vol. 2 1978.

[9] AA. Kamal, JB. Harness, G. Irving and AJ. Mearns, "Skin photoplethysmography a review," *Computer Methods and Programs in Biomedicine*, pp. 257-269, 1989.

[10] "Electric and Magnetic Measurement of the Electric Activity of the Heart," http://www.bem.fi/book/15/15.htm

[11] T. B. Garcia and N. E. Holtz, "12-Lead ECG: The Art of Interpretation," *Sudbury, Massachusetts, Jone and Bartlett,* 2001.

[12] D. Robotis, D. Huang and J. Daubert, "Head-up tilt-table testing: an overview. Annals of Noninvasive Electro cardiology," *Annals of Noninvasive Electrocardiology,* Volume 4, pp. 212-218, April 1999.

[13] G. Grassi and M. Esler, "How to assess sympathetic activity in humans," *Journal of hypertension*, pp. 719-734, 1999.

[14] H. Wellman and D. Zipes, "Cardiac sympathetic imaging with radioiodinated metaiodobenzy lguanidine (MIBG)," *Progress in Cardiology*, pp. 161-174, 1990.

[15] PK. Stein, MS. Bosner, RE. Kleiger and BM. Conger, "Heart rate variability: a mea-sure of cardiac autonomic tone," *American Heart Journal*, pp. 1376-1381, 1994.

[16] MT. La Rovere, GD. Pinna and A. Mortara, "Assessment of baroreflex sensitivity. In: Clinical guide to cardiac autonomic tests," *The Netherlands Kluwer Pulishers*, pp. 257-281, 1998.

[17] PJ. Schwartz and S. Wolf, "QT interval prolongation as predictor of sudden death in spatients with myocardial infarction," *American Heart Association, Circulation*, Volume 57, pp. 1074-1077, June 1978.

[18] G. Schmidt, M. Malik, P. Barthel, R. Schneider, K. Ulm, L. Rolnitzky, AJ. Camm, JT. Bigger and A. Schomig, "Heart rate turbulence after ventricular prematurebeats as a predictor of mortality after acute myocardial infarction," *The Lancet*, *Volume* 353, pp. 1390-1396, 1999.

[19] J. Sztajzel, "Heart rate variability: a noninvasive electrocardiographic method to measure the autonomic nervous system," *Swiss Medical Weekly, Volume* 134, pp. 514-522, 2004.

[20] S. Boonnithi and S. Phongsuphap, "Comparison of Heart Rate Variability (HRV) Measures for Mental Stress Detection," *Computing in Cardiology*, pp. 85-88, 2011.

[21] X. Chen., T. Chen, F. Luo and F. Li, "Comparison of Valley-to-Valley and Peak-to-Peak Intervals from photoplethysmographic Signals to Obtain Heart Rate Variability in the Sitting Position," *In Proceeding of International Conference on Biomedical Engineering and Informatic*s, pp. 214-218, 2013.

[22] S. Akselrod, D. Gordon, F.A. Ubel, D.C. Shannon, A.C. Barger and R.J. Cohen, "Power Spectrum Analysis of Heart rate Fluctuaton A Quqntitative Probe of Beat-to-Beat Cardiovascular Control," *Science, Volume* 213, pp. 220-222, 1981.

[23] R. L. Moses, "Introduction to Spectral Analysis," *Prentice-Hall Upper Saddle River, New Jersey* 07458, pp. 85-90, 1997.

[24] AB. Hertzman and CR. Spealman, "Observations on the finger volume pulse recorded photoelectrically," *American Journal of Physiology,* 1937.

[25] H. Molitor and M. A Kniazuk, "new bloodless method for continuous recording of peripheral circulatory changes," *Journal of Pharmacology and Experimental Therapeutics*, 1936.

[26] AB. Hertzman, "The blood supply of various skin areas as estimated by the photoelectric plethysmograph," *American Journal of Physiology*, pp. 328–340, 1938.

[27] AB. Hertzman and JB. Dillon, "Distinction between arterial, venous and flow components in photoelectric plethysmography in man," *American Journal of Physiology,* 1940.

[28] AB. Hertzman and JB. Dillon, "Applications of photoelectric plethysmography in peripheral vascular disease," *American Heart Journal*, 1940.

[29] T. Aoyagi, M. Kiahi, K. Yamaguchi and S. Watanabe, "Improvement of the earpiece oximeter," *Annual Meeting of the Japanese Society of Medical Electronics and Biological Engineering*, 1974.

[30] J. Allen "Photoplethysmography and its application in clinical physiological measurement," *Physiological Measurement*, *Volume* 28, pp. R1–R39, March 2007.

[31] S. Lu, H. Zhao, K. Ju, K. Shin, M. Lee, K. Shelley and H. Ki., "Can Photoplethy-smography variability serve as an alternative approach to be obtain heart rate variability information?," *Journal of Clinical Monitoring and Computing*, pp. 23-29, 2008.

[32] J. Hayano, A. K. Barros, A. Kamiya, N. Ohte and F. Yasuma, "Assessment of pulse rate variability by the method of pulse frequency demodulation," *BioMedical Engineering Online*, 2005.

[33] N. Selvaraj, A. K. Jaryal, J. Santhosh, K. K. Deepak and S. Anand, "Assessment of heart rate variability derived from finger-tip photoplethysmography as compared to electrocar-diography," *Journal of Medical Engineering & Technology*, 2008.

[34] K. Charlot, J. Cornolo, J. V. Brugniaux, J. P. Richalet and A. Pichon, "Interchangeability between heart rate and photoplethysmography variabilities during sympathetic stimulations," *Physiological Measurement*, 2009.

[35] W. A. Martin, E. Camenzind and P. R. Burkhard, “ECG artifact due to deep brain stimu-lation,” *The Lancet, Volume* 361, 2003.

[36] W. Chen, T. Kobayashi, S. Ichikawa, Y. Takeuchi and T. Togawa, “Continuous estimation of systolic blood pressure using the pulse arrival time and intermittent calibration,” *Medical & Biological Engineering & Computing, Volume* 38, pp. 69-74, 2000.

[37] H. Ma and Y. T. Zhang, “Spectral analysis of pulse transit time variability and its coherencewith other cardiovascular variabilities,” *Annual International Conference of the IEEE*, pp. 6442-6445, 2006.

[38] E. Gil, R. Bailion, J. M. Vergara and P. Laguna, “PTT variability for discrimination of sleep apnea related decreases in the amplitude fluctuations of PPG signal in children,” *IEEE Transaction on Biomedical Engineering, Volume* 57, pp. 1079-1088, May 2010.

[39] Y. Enze, H. Dianning, S. Yingfei, Z. Li, Y. Zhong and X. Lisheng, "Feasibility Analysis for Pulse Rate Variability to Replace Heart Rate Variability of the Healthy Subjects," *Proceeding of the IEEE International Conference on Robotics and Biomimetics*, pp. 1065-1070, 2013.

[40] M. Bolanos, H. Nazeran and E. Haltiwanger, "Comparison of Heart Rate Variability Signal Features Derived from Electrocardiography and Photoplethys-mography in Healthy Individuals*," Proceedings of the 28th IEEE, EMBS Annual International Conference New York City, USA*, pp. 4289-4294, 30 August, 2006.

[41] D. Nicholas, Giardino, M. Paul Lehrer and R. Edelberg, “Comparison of finger plethysmography to ECG in the measurement of heart rate variability. Psychophysiology,” *Psychophysiology*, pp. 246-253, 2002.

[42] E. Yu, D. He, Y. Su, L. Zheng and Z. Yin, "Feasibility Analysis for Pulse Rate Variability to Replace Heart Rate Variability of the Healthy Subjects," *Proceeding of the IEEE, International Conference on Robotics and Biomimetic*, pp. 1065-1070, 2013.

[43] E. Gil, M. Orini, R. Bail, J. M. Vergara, L. Mainardi and P. Laguna, "Photoplethy-smography pulse rate variability as a surrogate measurement of heart rate variability during non-stationary conditions," *Institute of Physics and Engineering in Medicine Printed in the UK*, pp. 1271-1290, 2010.

[44] A. V. J. Challoner, “Photoelectric plethysmography for estimating cutaneous blood flow,” *In Non-invasive Physiological Measurement, Oxford,* pp. 127-151, 1979.

Appendix

LIST OF PUBLICATIONS

International Conference Proceedings:

1. T. Sengthipphany, S. Tretriluxana and K. Chitsakul "Analysis of Heart Rate Variability and Breath to Breath Interval in Frequency Domain," *In proceeding of Biomedical Engineering International Conference*, IEEE, November 2014.
2. T. Sengthipphany, S. Tretriluxana and K. Chitsakul "Comparison of Heart Rate Statistical Parameters from Photoplethsmographic Signal in Resting and Exercise Conditions," *In proceeding of International Conference on Electrical Engineering/Electronics, Computer, Telecommunications and Information Technology*, IEEE, June 2015.

BMEiCON 2014

The 7th Biomedical Engineering International Conference

November 26-28, 2014

Fukuoka, Japan

IEEE Catalog Number (USB) : CFP1458R-USB **ISBN : 978-1-4799-6800-8**

Sponsor

IEEE Fukuoka Section 福岡支部

IEEE Advancing Technology for Humanity

IEEE West Japan Chapter EMB

IEEE Thailand Chapter EMB

Patrons

九州大学 KYUSHU UNIVERSITY

IEEJ

Analysis of Heart Rate Variability and Breath to Breath Interval in Frequency Domain

Tick Sengthipphany
Biomedical Measurement and Computation Laboratory
International college
King Mongkut's Institute of Technology Ladkrabang
Bangkok, Thailand
S6610018@kmitl.ac.th

Suradej Tretriluxana, Kitiphol Chitsakul
Biomedical Measurement and Computation Laboratory
Department of Electronics Engineering
Faculty of engineering
King Mongkut's Institute of Technology Ladkrabang
Bangkok, Thailand

Abstract— **Respiratory is known to be a confounding factor of Heart Rate Variability (HRV) analysis. This article introduces a Breath-to-Breath Interval (BBI) spectral computation to investigate the insight between respiration and the HRV. Six males and five female volunteers (age 20-25 years) underwent the Electrocardiogram (ECG) and respiratory chest movement recordings for 5 minutes while sitting in resting condition. Auto Regressive Moving Average (ARMA) model was employed to the R-wave to R-wave interval (RRI) and BBI signals for the spectral analysis. The results from all participants demonstrate that the peak amplitude in high frequency (0.15-0.40 Hz) band are higher than the ones in low frequency (0.04-0.15 Hz) band in both RRI and BBI frequency plots. It suggests that respiratory plays a major role in HRV oscillation. Our further study is to develop a mathematical model to explain this finding.**

Keywords— Heart rate variability (HRV); Breath to breath interval; frequency domain.

I. INTRODUCTION

Heart rate variability (HRV) is widely known as the quantitative measure of autonomic activity. HRV is influenced by a number of physiological and pathological conditions [7]. One of these is the respiration. It plays a major role in HRV oscillation as known as Respiratory Sinus Arrhythmia: (RSA) [10]. RSA is defined as the variability of heart rate due to the respiratory pattern. Studies [2, 3, 11] showed that there is a physical interaction between breathing cycle and cardiovascular system.

In frequency domain, the power spectrum of HRV analysis shows a low-frequency band (LF: 0.04–0.15 Hz) is reflecting sympathetic contributions (i.e., related to the "fight-or-flight" or stress response) and the high-frequency band (HF: 0.15–0.4 Hz) is usually considered as a marker of parasympathetic activity, which occurs when the body is at rest [13].

Many researchers consider the LF area to involve sympathetic activity, however, some studies show that the LF area corresponds to both sympathetic and parasympathetic activities. The respiration has a significant effect on the heart rate oscillations at the frequency close to the respiratory sinus rhythm [2, 3, 4, 10, 12]. Recent studies have shown that respiratory peak could be used as a quantitative measure of vagal control.

In this study, the spectral analysis by using the AutoRegressive Moving Average (ARMA) model on the RRI and BBI was performed. The frequency characteristic of both signals is investigated [14]. The revealed the information might lead to the new knowledge that explain the physiological mechanism between respiration and HRV.

II. METHODS

A. Experimental protocol

ECG and breathing signals from eleven healthy volunteers were collected (6 male, 5 female; age AGE±SD years), while the subjects performed normal breathing for approximately 5 minutes. Both signals were digitized at 250Hz sampling frequency and stored in a computer. RR intervals were detected from the ECG, and BB interval was detected from the breathing signal.

B. Signal acquisition and preprocessing

ECG and breathing signals were continuously acquired with the subjects sitting. The ECG and respiration belts were connected to a multi-modality device for real-time computerized (The BioHarness operates in Bluetooth transmitting of data to AcqKnowledge software using the universal serial bus (USB) docking for receiving data and then save the data as a computer) and data acquisition (Bioharness device with acknowledge software Biopac). Every channel was acquired at 250 Hz sampling rate. The ECG and breathing signal were analyzed with custom software development using the LabVIEW™ 2011 program in order to detect the R peaks and calculate the RR series as the time interval between two consecutive R peaks, detected by a traditional derivative threshold procedure. The

978-1-4799-6801-5/14/$31.00 ©2014 IEEE

Breathing signal was low-pass filtered for help smooth signal, breath to breath interval (BBI) was detected from a peak of breathing.

For peak detector, Is finding the location in time series t(i), and second derivative of peaks in the input signal. (i = 1,2,3,....,n), use the following equation.

$$RR(i) = t(i) - t(i-1) \quad (1)$$

C. Frequency domain analysis

Spectral analysis was performed and prediction by Autoregressive Moving Average (ARMA) spectral methods. Time Series Analysis (TSA) ARMA Modeling estimates the Autoregressive Moving Average (ARMA) model of an input variable time series according to the method we specify. And the order was chosen between 12 to 25, The visual instrument (VI) computes the spectral density based on autoregressive-moving average (ARMA) modeling according to the following equation:

$$Z(f) = \frac{\sigma^2 \left| \sum_{k=0}^{N-1} y'(k) \exp(\frac{-j2\pi kf}{f_s}) \right|^2}{df \left| \sum_{k=0}^{N-1} x'(k) \exp(\frac{-j2\pi kf}{f_s}) \right|^2} \quad (2)$$

Where Z (*f*): Is the PSD of the time series:

- *df* : Is the frequency interval
- σ^2 : Is the estimated noise series of the ARMA model of the time series
- exp: Is computes the base e exponential of the input elements

Which is computed as f_s /*N*:

- *N*: Is the number of frequency bins
- f_s: Is the sampling rate
- x: Is an array that contains the AR coefficients of the ARMA(*m*, *n*) model, and *x*= [1,x_1, x_2,…,x_m]
- y: Is another array that contains the MA coefficients of the ARMA(*m*, *n*) model, and y= [1,y_1,y_2,…, y_n]
- Before computing the PSD, this VI wraps x, y to *N*-point series x', y'.

The spectral analysis brings to predict the two components of the autonomic nervous system (ANS), sympathetic and parasympathetic, increase or decrease the heart rate and influence different bands in the spectrum of RR intervals and BB intervals. The spectrum of the HRV signal is generally calculated either from the RR interval tachogram (RR durations with a number of progressive beats) using Autoregressive Moving Average (ARMA) spectral methods [13,14] and We were this method of respiration too. In the frequency on table 1, The figure 1 and figure 2 are the Block diagram for ECG and breathing processing using the Labview program

TABLE 1. FREQUENCY-DOMAIN MEASUREMENTS OF HRV [13]

No	Analysis of short-term recording		
	Variable	***Unit***	***Description***
1	VLF	ms^2	Power from 0 Hz to 0.04 Hz
2	LF	ms^2	Power from 0.04 Hz to 0.15 Hz
3	HF	ms^2	Power from 0.15 Hz to 0.4 Hz

VLF: Very low frequency LF: low frequency; HR: High frequency

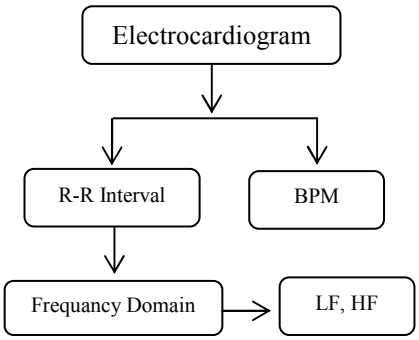

Figure 1: Block diagram for electrocardiogram processing in Labview program

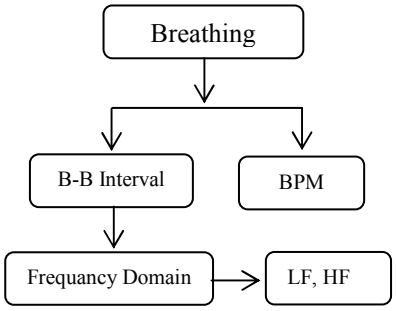

Figure 2: Block diagram for breathing processing in Labview program

III. RESULTS

We have a preliminary frequency domain analysis of electrocardiogram (ECG) and the breathing signals at normal condition. Figure 3 (a) show an Electrocardiogram (ECG) and marker of peak detector, Figure 3 (b) The peak to peak interval (RRI) from Electrocardiogram (ECG), Figure 3 (c) show a Breathing signal and mark of peak detector, Figure 3 (d) The breath-to-breath interval (BBI) from breathing signal. Figure 4 is the spectrum of the HRV and the respiration signal obtained from the frequency domain plot at frequency. They are close to the HF and LF areas as it can be seen from the figure. HRV and respiration indicate the HF area as a measure of parasympathetic. However the parameter in LF and HF of HRV and respiration are not synchronous. Prediction of ARMA model.

This is an expected result from parasympathetic activity is mediated by breath-to-breath interval (BBI). On the other hand, in HRV analysis, HF power would be located in the interval 0.15-0.4 Hz where there is almost show power (Figure 4 The results of analyzing the HRV and BBI signal from ECG signal and the breathing signal in the frequency domain analysis of all 11 subjects are displayed in table 2: is show the parameter of frequency and table 3: is show the parameter of PSD. Although mean values of beat per minute (BPM), low frequency (LF), high frequency (HF). An expected increase in HF power (Parasympathetic measurement) by HRV and BBI analysis.

(a)

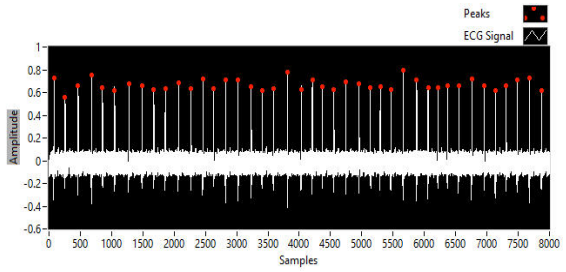

(b)

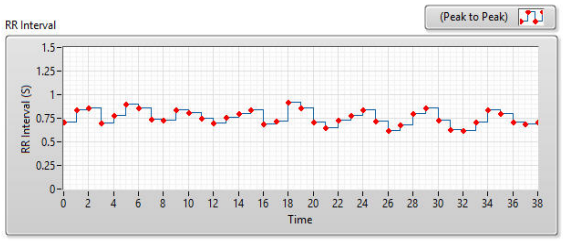

(c)

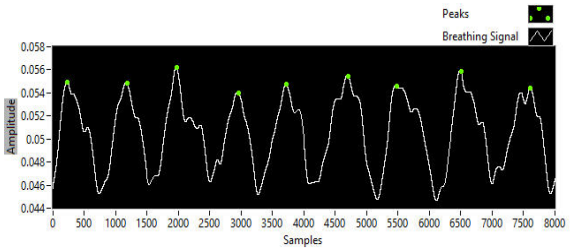

(d)

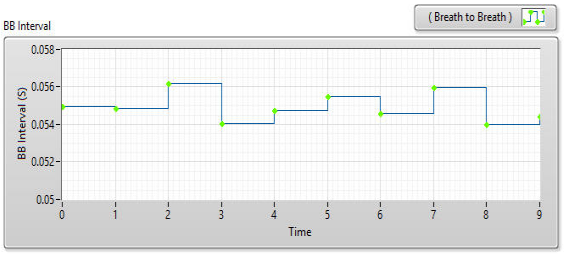

Figure 3: (a), (c) Example an ECG and a breathing signal with the same sampling rate and detect peak, (b) is peak to peak interval (RRI) from ECG signal and, (d) is breath-to-breath interval (BBI) from breathing signal.

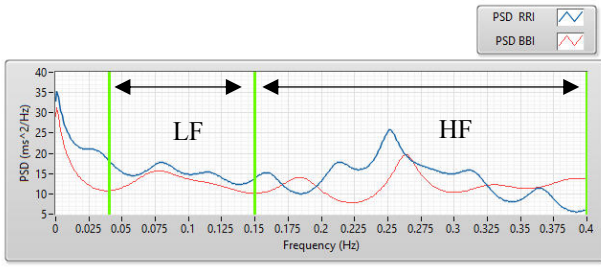

Figure 4: Subject1 (S1) Frequency domain analysis of HRV and BBI of ECG signal and breathing signal for 5 minutes.

In Figure 4 is shown an isolation area of high and low frequency power (LF: 0.04 to 0.15Hz, and HF: 0.15 to 0.4Hz region) is very clear. HRV and BBI indicate the HF area as a measure of parasympathetic. In this figure we could see the Power Spectral Density (PSD) in Y-axis of high frequency all of HRV, Breathing from RRI and BBI have parameter higher than low frequency. From this is meant the variation in RRI and had corresponded with BBI to consider as markers of parasympathetic activity, which occurs when the body is at rest.

TABLE2.PARAMETEROF FREQUENCY FROM FREQUENCY DOMAIN ANALYSIS.

No	Analysis of short-term recording					
	HR *(BPM)*	***Breathing*** *(BPM)*	***HRV***		***BBI***	
			LF (Hz)	***HF (Hz)***	***LF (Hz)***	***HF (Hz)***
S1	67	25	0.08	0.34	0.145	0.225
S2	87	12	0.14	0.16	0.15	0.25
S3	84	9	0.08	0.16	0.1	0.16
S4	76	12	0.15	0.19	0.045	0.22
S5	65	18	0.08	0.29	0.14	0.35
S6	61	19	0.08	0.26	0.06	0.26
S7	54	13	0.08	0.25	0.075	0.037
S8	82	17	0.09	0.29	0.09	0.29
S9	65	15	0.07	0.24	0.1	0.35
S10	72	18	0.06	0.24	0.06	0.2
S11	70	15	0.05	0.225	0.098	0.267

BPM: beat per minute; BBI:breath-to-breath interval; HRV: heart rate variability; HR: heart rate; LF: low frequency; HR: High frequency; S1 to S11: Subject 1 to Subject 11

TABLE 3. PARAMETER OF PSD FROM FREQUENCY DOMAIN ANALYSIS.

No	Analysis of short-term recording			
	HRV		***BBI***	
	LF *(ms^2/Hz)*	***HF*** *(ms^2/Hz)*	***LF*** *(ms^2/Hz)*	***HF*** *(ms^2/Hz)*
S1	23	28	20	22
S2	28	28.6	17.5	20

No	Analysis of short-term recording			
	HRV		*BBI*	
	LF *(ms^2/Hz)*	***HF*** *(ms^2/Hz)*	***LF*** *(ms^2/Hz)*	***HF*** *(ms^2/Hz)*
S3	23.4	24	20	21.6
S4	31	32.9	15	29
S5	20	25	20.2	21
S6	21.4	29	25	38
S7	16.3	24.9	14.9	17
S8	24.3	28	24.3	40
S9	24	20	20	20.2
S10	26.3	24	20	23
S11	25	24.2	20	29

HRV: heart rate variability; BBI:breath-to-breath interval; LF: low frequency; HR: High frequency; S1 to S11: Subject 1 to Subject 11

IV. Discussion and Conclusion

The objective of this study was to investigate the mechanism between breathing and HRV [1, 8]. Applying the ARMA model allow us to extract frequency information from the autonomic function and breathing pattern. A sample plot from one of the participant data is illustrated in figure 4. Both PSD (ms^2/Hz) and frequencies (Hz) from the highest peaks in two bands are summarized in table 2 and 3.

The summary result from table 2 and 3 shows that the parameter in LF and HF of between HRV and BBI are not synchronous. Whatever, In the figure we can find significant differences for coherence of PSD in Y-axis, between high frequency and low frequency as shown in figure and table of parameter by RRI and BBI power spectral analysis and have got a parameter of PSD in high frequency higher than low frequency that indicates the influence of the parasympathetic component of autonomic nervous system (ANS). However, further research is needed to confirm these interesting findings. So we need more conditioner and subject to confirm this hypothesis.

In conclusion, this paper introduced the new respiratory signal, Breath-to-Breath Interval. By using the parametric ARMA model, we computed the RRI and BBI frequency spectrums and searched for the relation between two plots Our results show that the peak amplitudes in HF band is higher than the ones in the LF band on both RRI and BBI plots. This suggests that respiration makes more contribution in the HF band. This is also a confirmation of the role of RSA in the HRV. To explain this finding, the mathematical model is developed in the future.

The processing and analysis of electrocardiography and breathing signals has been presented. Methods in frequency domains that was used to detect the parameters of heart rate variability and breath to breath interval to study the correlation of defined portions of High frequency to predict the parasympathetic activity. The frequency analysis has shown the relationship between a breath to breath (BBI) and heart rate variability (HRV) frequency during an uncontrolled condition.

Acknowledgment

We would like to thank our participants in this study. We also grateful to graduate students in Biomedical Measurement and Computation Laboratory (BMCL) for help and discussion and We would like to thank the AUN/SEED-Net for the financial support to Miss Tick Sengthipphany to study at King Mongkut's Institute of Technology Ladkrabang (KMITL), Bangkok, THAILAND..

References

[1] E. Barrera C, M.A. Fabian A and H. Ruiz V, "Processing of ECG and Breathing Signals to Study the Correlation of Respiration Waveform Time Intervals with HF and LF Powers of Heart Rate Variability" IEEE computer society, 2008, pp. 592-597

[2] Benhur Aysin, Elif Aysin, "Effect of Respiration in Heart Rate Variability (HRV) Analysis," New York City, Aug 30-Sept 3,2006, pp. 1776-1779, IEEE.

[3] Thuraia M. Alkhoori, Habiba S. Alsafar, Ahsan H. Khandoker, "Analysis between ECG and Respiration Signals in Type II Diabetic Patients in the UAE" 2014, pp. 346-348

[4] V Magagnin, M Mauri, P Cipresso, L Mainardi, EN Brown, S Cerutti, M Villamira, and R Barbieri, "Heart Rate Variability and Respiratory Sinus Arrhythmia Assessment of Affective States by Bivariate Autoregressive Spectral analysis" Computing in Cardiology 2010, pp. 145-148, ISSN

[5] A. Espíritu Santo, C. Carbajal "Respiration Rate Extraction from ECG Signal via Discrete Wavelet Transform" IEEE 2010

[6] K. Venu Madhav1, M. Raghu Ram2, E. Hari Krishna3, Nagarjuna Reddy Komalla4 , K. Ashoka Reddy5, "Estimation of Respiration Rate from ECG, BP and PPG signals using Empirical Mode Decomposition" IEEE 2011,

[7] Golosarsky, B. Can heart rate variability timing reflect the body stress?. Med hypotheses 2006 V 67, 6, 1467-1468.

[8] V. Demchenko, R. Cmejla, and J. Vokral, " Analysis of heart rate variability during respiration"

[9] Jongyoon Choi, and Ricardo Gutierrez-Osuna, "Removal of Respiratory Influences From Heart Rate Variability in Stress Monitoring" IEEE 2011, pp. 2649-2656

[10] J. D. Schipke, M. Pelzer, G. Arnold "Effect of respiration rate on short-term heart rate variability" 1999, pp. 92-95

[11] Sandun Kodituwakku, Sara W Lazar, Premananda Indic, "Point Process Time-Frequency Analysis of Respiratory Sinus Arrhythmia under Altered Respiration Dynamics" IEEE 2010, pp. 1622-1625

[12] P. Grossman,1 F. H. Wilhelm,2 and M. Spoerle1, "Respiratory sinus arrhythmia, cardiac vagal control, and daily activity" the American Physiological Society, 2004, pp. 728-734

[13] "Heart rate variability Standards of measurement, physiological interpretation, and clinical use: Task Force of The European Society of Cardiology and The North American Society of Pacing and Electrophysiology (Membership of the Task Force listed in the Appendix) "American Heart Association Inc.; European Society of Cardiology, 1996, pp. 354-381

[14] S. Akselrod and et al "Power Spectrum Analysis of Heart rate Fluctuaton A Quqntitative Probe of Beat-to-Beat Cardiovascular Control" Science, 213, pp 220-222, 1981

[15] Y. Fumihiko and H. Jun-ichico " Respiratory Sinus Arrhythmia: Why does the heartbeat synchronize with respiratory rhythm?" Chest, 125, pp 685-690, 2004

ECTI-CON 2015

June 24 - 27, 2015

2015 12 International Conference on Electrical Engineering/Electronics, Computer, Telecommunications and Information Technology

NBTC

PEA

IEEE THAILAND SECTION

ECTI Association

Comparison of Heart Rate Statistical Parameters from Photoplethysmographic Signal in Resting and Exercise Conditions

T. Sengthipphany
Biomedical Measurement and Computation Laboratory
International college
King Mongkut's Institute of Technology Ladkrabang
Bangkok, Thailand
S6610018@kmitl.ac.th

S. Tretriluxana, K. Chitsakul
Biomedical Measurement and Computation Laboratory
Department of Electronics Engineering
Faculty of engineering
King Mongkut's Institute of Technology Ladkrabang
Bangkok, Thailand

***Abstract*— The aim of this article is to investigate the possibility of computing Heart Rate Variability (HRV) indices from the finger Photoplethysmogram. To indicate that whether Pulse Rate Variability (PRV) from PPG signal can be used as an alternative to Heart Rate Variability (HRV) from ECG signal. The Photoplethsmographic (PPG) and Electrocardiographic (ECG) signals from 33 participants were recorded simultaneously during resting and exercise conditions. The peaks of PPG and R-waves of ECG were detected and reconstructed to the Peak-to-Peak interval (PPI) and R-to-R interval (RRI) waveforms respectively. In both conditions, the mean and standard deviation (SDNN) of the intervals over 5 minutes were computed from the two waveforms. Results from cross correlation between PPI and RRI show that the average correlation coefficients (r) are higher in resting than the "r" in exercise. In regression analysis of the statistical parameters between RRI and PPI, the determination coefficients (R^2) of the means are close to one in both conditions, whereas the R^2 of SDNN in exercise is lower than the one in resting. This finding suggests that the HRV indices can be evaluated from PPG with reliability during the rest.**

Keywords—Heart Rate Variability (HRV), Photoplethysmography, Electrocardiogram (ECG), Heart Rate (HR), Cardiac Autonomic Function.

I. INTRODUCTION

Heart Rate Variability (HRV) is well known to be the measure of cardiac autonomic function. The two branches of systemic control, sympathetic and parasympathetic (vagal) modulations, are reflected in the variation of heart beat interval in Electrocardiogram (ECG) [2,4]. HRV has been used in a large number of research to study physiological and psychological dysfunctions. Though it gains popularity as the noninvasive marker, the setup of ECG recording is sometimes inconvenient, particularly in study with movement activities.

Photoplethysmography (PPG) is a simple and widely used technique for measuring changes in blood volume. The finger photoplethysmography is often found anywhere inform of a portable stand alone unit or part of the sophisticated bedside monitor system. In clinic, the primary function of PPG device is to monitor arterial oxygen saturation (SaO_2). PPG signal also provides valuable information of cardiac autonomic activity via the pulsatile waveform [8]. The samples of simultaneously recorded ECG and PPG are given in Fig. 1.

Photoplethysmography (PPG) has been considered as a promising surrogate for electrocardiography (ECG) in measuring heart rate variability (HRV). The High correlation between pulse intervals and RR intervals (RRI) were obtained in some studies, and it was concluded that pulse variability can serve as an alternative approach to obtain HRV information [3,6,7,9]; However, there stood only resting condition. So in our work we use the rest and Exercise condition for this research, To study the HRV from PP Intervals of Photoplethysmographic (PPG) and RR intervals of Electrocardiographic (ECG) signals.

In this paper, the beat-to-beat interval waveforms extracted from PPG and ECG were generated. The cross correlation between two waveforms were evaluated during resting and exercise. In addition, we computed two statistical parameters, mean and standard deviation, of heart rate (HR) based on those waveforms. They are two fundamental parameters for computing HRV indices. Finally, both parameters were compared by regressing analysis.

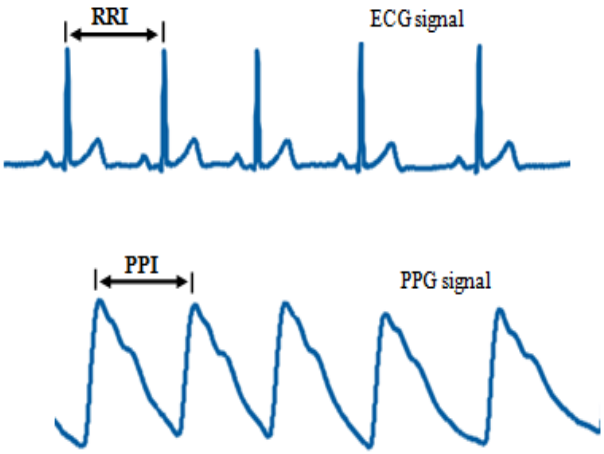

Fig. 1. The samples of ECG and PPG signals

978-1-4799-7961-5/15/$31.00 ©2015 IEEE

II. MATERIALS AND METHODS

A. Subjects

Thirty three biomedical engineering students (20 males and 13 females) participated in this study. Their demographics (mean±SD) are presented in Table I.

TABLE I. DEMOGRAPHICS OF PARTICIPANTS

No. of Participants	*Age (year)*	*Height (cm)*	*Weight (kg)*
33	21.34±1.42	168.28±8.05	67.87±12.6

B. Data Acquision and Experiment Protocol

Each participant was equipped with an optical transducer for recording the PPG at the fingertip (Fig. 2) and three surface electrodes were placed on the body for ECG (lead II) monitoring [10]. All sensors were connected to an Analog-to-Digital Converter unit (MP36 Biopac Systems Inc., Santa Barbara, CA, USA, Fig. 3). Data were displayed and stored at 500Hz sampling frequency in the computer for the off-line analysis.

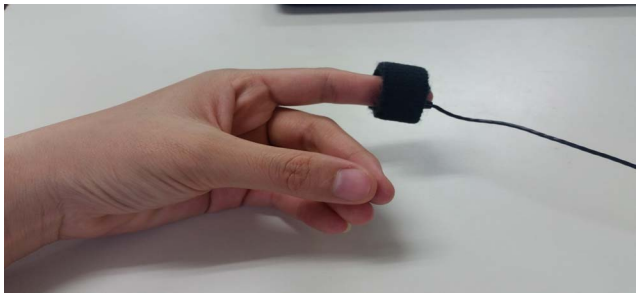

Fig. 2. The Finger photoplethysmogram (PPG) transducer

Fig. 3. The Analog-to-Digital unit Biopac MP36

The experiment, trial is divided into two parts, resting and an exercise. Participants were first asked to lie down with eyes closed (Fig. 4) in a quiet room for 10 minutes. They were, in the next 15 minutes, doing exercise on a stationary bicycle (Fig. 5) to make their HR higher than 130 beats/minute continuously for at least 5 minutes.

Fig. 4. Participant in resting condition

Fig. 5. Exercise condition on Stationary Bicycle

C. Data Analysis

For each trial, the two 5-minute portion of PPG and ECG were selected from resting and exercise conditions as demonstrated in Fig 6. Due to the poor signal quality, four subject's data were removed from the analysis in exercise conditions. All peaks of PPG and R-waves of ECG were detected and reconstructed to Peak-to-Peak (PPI) and R-to-R interval (RRI) time series respectively (Fig.7). The cross correlations between these two time series were performed and two average correlation coefficients (r) were computed across subjects in resting (n=33 in Fig.8) and exercise (n=29 in Fig.9) conditions.

Two statistical parameters, mean and Standard Deviation of Normal-to-Normal interval (SDNN) [1] were computed on the two 5-minute time series in both conditions. Regression analyses were performed between the same parameters derived from PPI and RRI in two conditions. Four determination coefficients (R^2) are calculated and shown in Fig. 10.

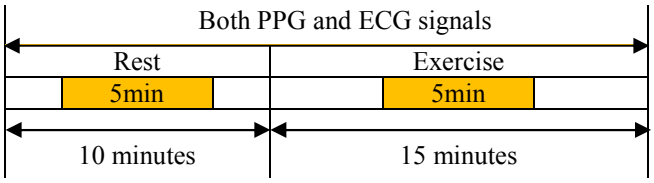

Fig. 6. Selected 5-minute portions from both conditions

D. Correlation of RR interval and PP interval

The correlation between RR interval and PP interval, We use correlation coefficient and the coefficient of determination methods to indicate a correlation.

The linear correlation coefficient also is known as the Pearson's correlation. The following equation describes the linear correlation coefficient:

$$r = \frac{n(\sum xy) - (\sum x)(\sum y)}{\sqrt{[n(\sum x^2) - (\sum x)^2] \times [n(\sum y^2) - (\sum y)^2]}} \quad (1)$$

Correlation coefficient r always is in the interval [–1, 1]. If correlation coefficient r is 1, X and Y have a complete positive correlation. In other words, the data points from X and Y lie on a perfectly straight, positively-sloped line. If correlation coefficient r is –1, X and Y have a complete negative correlation. In other words, the data points from X and Y lie on a perfectly straight, negatively-sloped line. If correlation coefficient r is 0, X and Y have no correlation, n is sample size.

The coefficient of determination is the ratio of the explained variation to the total variation. The coefficient of determination is such that $0 < R^2 < 1$, and show the strength of the linear association between x and y. The coefficient of determination represents the percent of the data that is the closest to the line of best fit.

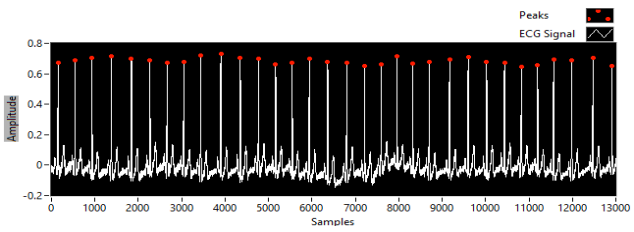

(a)

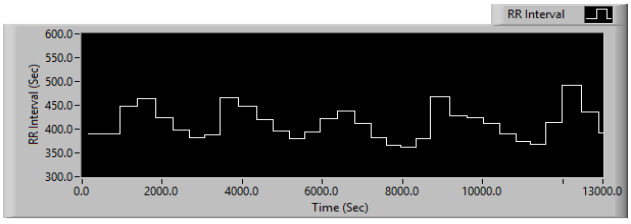

(b)

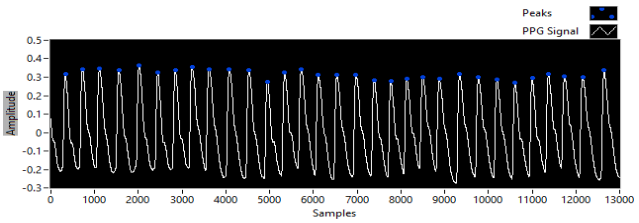

(c)

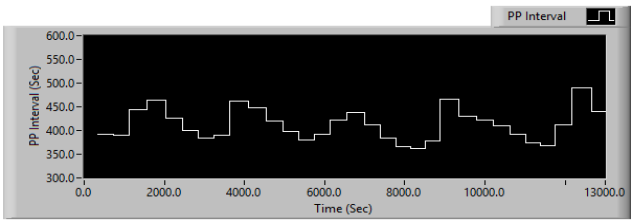

(d)

Fig. 7. (a) Sample of ECG signal ,(b) RRI signal derived from ECG, (c) Sample of PPG signal, (d) PPI signal derived from PPG.

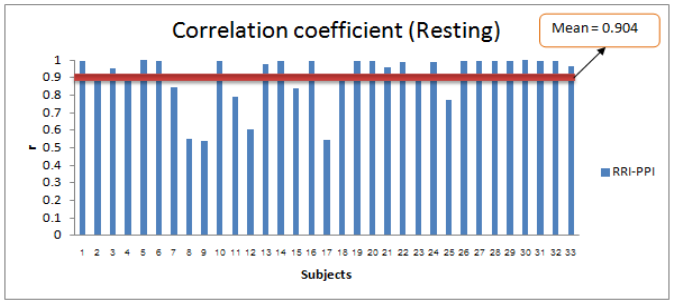

Fig. 8. The correlation coefficients, *r*, between the RRI and PPI during resting state (n=33, the average '*r*' is 0.904)

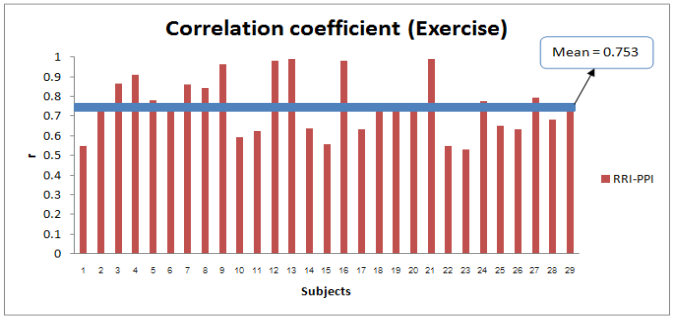

Fig. 9. The correlation coefficients, *r*, between the RRI and PPI during exercise (n=29, the average '*r*' is 0.753)

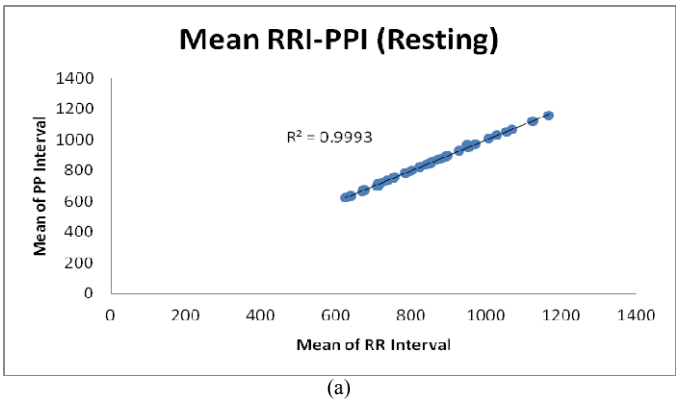

(a)

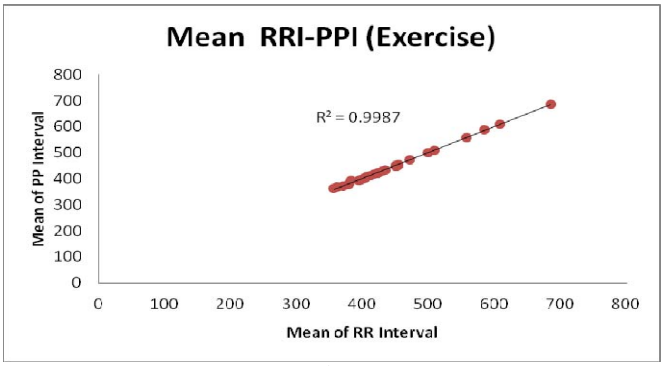

(b)

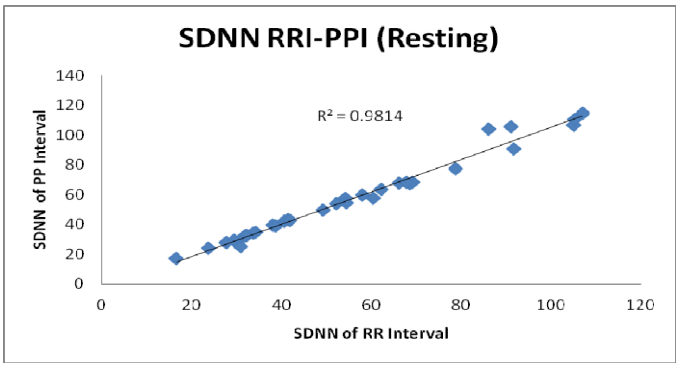

(c)

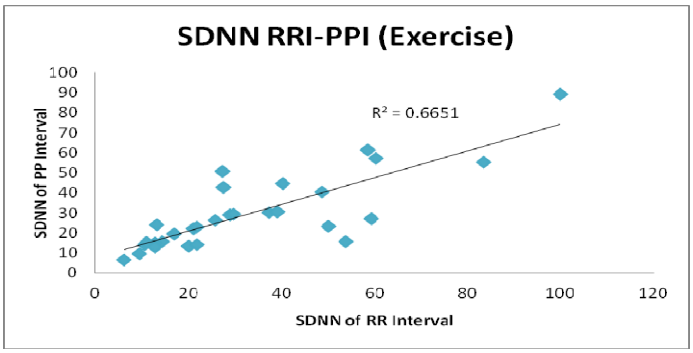

(d)

Fig. 10. The determination coefficient, R^2, regression analysis (a). between two means in resting state, (b). between two means during exercise, (c). between two SDNNs in resting state, (d). between two SDNNs during exercise.

III. Results

The average correlation coefficients (r) between PPI and RRI in resting is 0.904, higher than the average "r" between PPI and RRI during exercise (0.753). Table II summarizes the four determination coefficients (R^2) generated by regression analyses between the same parameters derived from PPI and RRI.

TABLE II. Determination coefficients (R^2) of Mean, SDNN

Condition	Mean	SDNN
Resting	0.9993	0.9814
Exercise	0.9987	0.6651

IV. Discussion and Conclusion

The average value of "r" calculated from the cross correlation between PPI and RRI suggests that these two beat-to-beat interval time series are consistent with higher degree in resting than exercise. Supported by the evidence of R^2 from regression analysis of statistical parameters in Table II, the bigger numbers (R^2 of mean and SDNN) are reported in resting. All lower indicators in exercise are due to the quality of acquired signals. And In rest condition the result has the close value with other research from the correlation coefficient and the coefficient of Determination calculated [3,9]. So the PP intervals from PPG signal can be used as an alternative to Heart Rate Variability (HRV) from the ECG signal in both the rest and exercise condition. However, during the exercise condition depends on the applications.

Usually, the fluid dynamic of blood circulation, cardiac arrhythmia and blood vessel's compliance play a key role in PPG fluctuation. The movement artifact, however, can seriously contaminate both PPG and ECG during exercise. Fig 11 and 12 demonstrate samples of the ECG and PPG during exercise with undetected peaks. These irregular patterns make difficulty to correctly find the peaks and lead to erroneous beat-to-beat waveform formation.

Physiologically, ECG and PPG are both originated from the cardiovascular system. They are in fact generated from different mechanisms. Cardiac pacemaker is electrically monitored by ECG while the PPG is the result of mechanical wave (blood pressure) travelling from the left ventricle to the finger. Their variabilities of HR are expectedly identical. Our study concludes that HRV indices can be calculated with confidence from PPG during the resting state. The inconsistent value, R^2 of SDNN, during exercise is the consequence of poor PPG and ECG signal quality causing incorrect peak detection. An alternative technique to better identify the beat-to-beat interval is needed. The study showed valley-to-valley interval of PPG gives higher accuracy than the peak-to-peak detection. [9]. This will be part of our development.

An interest in wearable technology brings an attention to photoplethsmogram. To assess long term HRV analysis, PPG's beat intervals gain more attraction than ECG's counterparts. As a compact, non-invasive, multipurpose

device, finger plethsmographaph is future health care self monitoring solution.

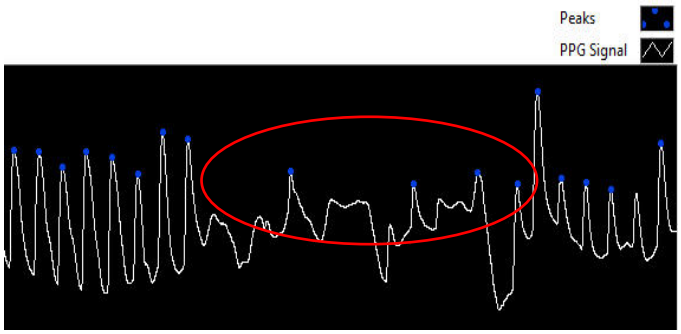

Fig. 11: Sample of contaminated PPG during exercise

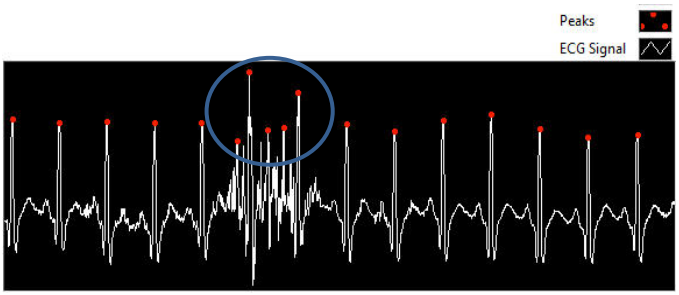

Fig. 12: Sample of contaminated ECG during exercise

ACKNOWLEDGMENTS

We would like to give acknowledgments to King Mongkut's Institute of Technology Ladkrabang Research Fund and AUN /SEED-Net program for scholarship. We thank all participants in this research and are also grateful to the members of Biomedical Measurement and Computation Laboratory (BMCL) for help.

REFERENCES

[1] "Heart rate variability Standards of measurement, physiological interpretation, and clinical use: Task Force of The European Society of Cardiology and The North American Society of Pacing and Electrophysiology (Membership of the Task Force listed in the Appendix) "American Heart Association Inc.; European Society of Cardiology, 1996, pp. 354-381

[2] S. Boonnithi, S. Phongsuphap, "Comparison of Heart Rate Variability (HRV) Measures for Mental Stress Detection", Computing in Cardiology 2011, pp: 85-88

[3] Sheng Lu, PhD, He Zhao, MS, Kihwan Ju, PhD, Kunsoo Shin, PhD, Myoungho Lee, PhD, Kirk Shelley, PhD and Ki H. Chon, PhD, "Can Photoplethysmography variability serve as an alternative approach to be obtain heart rate variability information?" Journal of Clinical Monitoring and Computing , 2008, pp. 23-29

[4] "Heart rate variability: a noninvasive electrocardiographic method to measure the autonomic nervous system", Cardiology Center and Medical Policlinics, University Hospital, Geneva, Switzerland, 2 0 0 4, pp. 514-522

[5] Enze Yu, Dianning He, Yingfei Su, Li Zheng, Zhong Yin, Lisheng Xu, "Feasibility Analysis for Pulse Rate Variability to Replace Heart Rate Variability of the Healthy Subjects" 2013, pp. 1065-1070, IEEE

[6] M. Bolanos, H. Nazeran, E. Haltiwanger, "Comparison of Heart Rate Variability Signal Features Derived from Electrocardiography and Photoplethysmography in Healthy Individuals" New York City, USA, Aug 30-Sept 3, 2006, pp. 4289-4294

E. Gil, M. Orini, R. Bailon, J. M. Vergara, L. Mainardi and P. Laguna, "Time-varying spectral analysis for comparison of HRV and PPG variability during tilt table test" 2010, pp: 3579-3582, IEEE

[7] Nicholas D. Giardino, Paul M. Lehrer, Robert Edelberg, "Comparison of finger plethysmography to ECG in the measurement of heart rate variability. Psychophysiology", 2002; 39 (2): 246-253.

[8] E. Gil, M. Orini, R. Bail, J. M. Vergara, L. Mainardi and P. Laguna, "Photoplethysmography pulse rate variability as a surrogate measurement of heart rate variability during non-stationary conditions" Institute of Physics and Engineering in Medicine Printed in the UK 2010, pp. 1271-1290

[9] Xiang Chen, Tianjun Chen, Feifei Luo, Jin Li, "Comparison of Valley-to-Valley and Peak-to-Peak Intervals from Photoplethysmographic Signals to Obtain Heart Rate Variability in the Sitting Position" 2013, pp. 214-218, IEEE

[10] Garcia, T.B., Holtz, N.E., 12-Lead ECG: The Art of Interpretation, Sudbury, Massachusetts, Jone and Bartlett Publishers, 2001.

AUTHOR BIOGRAPHY

NAME	Miss Tick Sengthipphany
STUDENT ID	56610018
DATE OF BIRTH	October 13, 1989
ADDRESS	Khai vieng, Kham District, Xiengkhouang Provine, Laos
EDUCATIONAL	She received her Bachelor degree in Electronic engineering in 2012 from the Department of Electronic and Telecommunication Engineering, Faculty of Engineering, National University of Laos. Currently, she is a Master Candidate under the ASEAN University Network/Southeast Asia Engineering Education Development Network (AUN-SEE/Net) program in major of Computing in Engineering System, International College, King Mongkut's Institute of Technology Ladkrabang, Bangkok, Thailand.